Ramanujan Holographic Scanning Principle: Modular Curves, Hecke Dynamics, and an Arithmetic Constitution for HPA–Ω

Haobo Ma (Auric)*
AELF PTE LTD.
#14-02, Marina Bay Financial Centre Tower 1, 8 Marina Blvd, Singapore 018981

January 1, 2026

Abstract

There is a long-standing tension between the continuous, reversible nature of quantum unitarity and the discrete, finite-resolution character of observed outcomes. This paper proposes an auditable and reproducible *arithmetic–holographic–computational constitution*: not an engineering design, but a minimal dependency chain from arithmetic geometry (modular curves, modular forms, and Hecke operators) to the HPA–Ω scan–projection readout architecture.

The organizing constraints are finite information and holographic encoding. We define *time* as the iteration count of an intrinsic unitary scan; *probability* as an induced measure produced by finite-resolution projection readout, rather than an externally postulated sampling rule; and *discreteness* as integer Fourier data generated by q-expansions at cusps. The core claim is that the modular flow on the modular curve $X(1)$ provides a natural geometric mother space for scan dynamics, the Hecke algebra supplies a symmetry-preserving cross-scale renormalization skeleton generated by primes, and continued-fraction/Ostrowski coding (specializing to Zeckendorf on the golden branch) provides a canonical interface between integer time and bit-level readout.

At the level of modular data, we also emphasize the classical Ramanujan differential system as a canonical q-flow on the distinguished generators, making the "cusp interface" not only a source of discrete coefficients but also a rigid differential calculus. Interpretation-layer viewpoints are explicitly segregated and do not enter the Layer 0/1 closure.

Keywords: arithmetic geometry, modular forms, quasi-modular forms, Ramanujan differential equations, Hecke operators, modular curve, holography, unitary scan, Weyl pair, Ostrowski/Zeckendorf coding, Sturmian/Fibonacci words, induced measure, HPA, Omega Theory.

Conventions. Unless otherwise stated, log denotes the natural logarithm. "mod 1" refers to reduction in $\mathbb{R}/\mathbb{Z}$. "Tick time" $t \in \mathbb{Z}_{\geq 0}$ denotes the iteration count of a scan operator. When convenient, we freely replace $[0, 1)$ by $[0, 1]$ in integrals and discrepancy definitions, since the boundary has Lebesgue measure zero.

Contents

*Email: auric@aelf.io

1 Introduction: the continuous–discrete tension and the role of a "constitution"

> *Chaos is merely a matter of perspective. Viewed from the cusp, the universe is a single, straight vector of light.*
> *The universe is a prism. Data is scattered light. Computation is the lens that refocuses it back to the source.*[1]

Modern foundational physics confronts a structurally persistent mismatch:

- **Dynamics layer**: quantum theory is organized around unitary evolution—continuous, reversible, and information-preserving.
- **Readout layer**: observation presents discrete outcomes—counts, bits, integer labels, and finite-precision statistics.

Standard treatments delegate continuity to an ontic object (Hilbert space, fields) and discreteness to measurement postulates (projection, POVMs) plus external probabilistic interpretation. Here we invert the emphasis: *readout is treated as part of physical structure*, and we demand a closed, minimal dependency chain in which *time/probability/discreteness* are not external semantics but endogenous objects of a scan–projection protocol.

This manuscript is written as a *mathematical constitution*. The goal is not to assert an experimentally complete physical law, but to provide an auditable chain of definitions and standard theorems that connects:

$$\begin{aligned} &\text{modular action} \Rightarrow \text{cusp } q\text{-expansion} \Rightarrow \text{discrete coefficients} \\ &\qquad \Rightarrow \text{Hecke/prime skeleton} \Rightarrow \text{canonical coding}. \end{aligned} \tag{1}$$

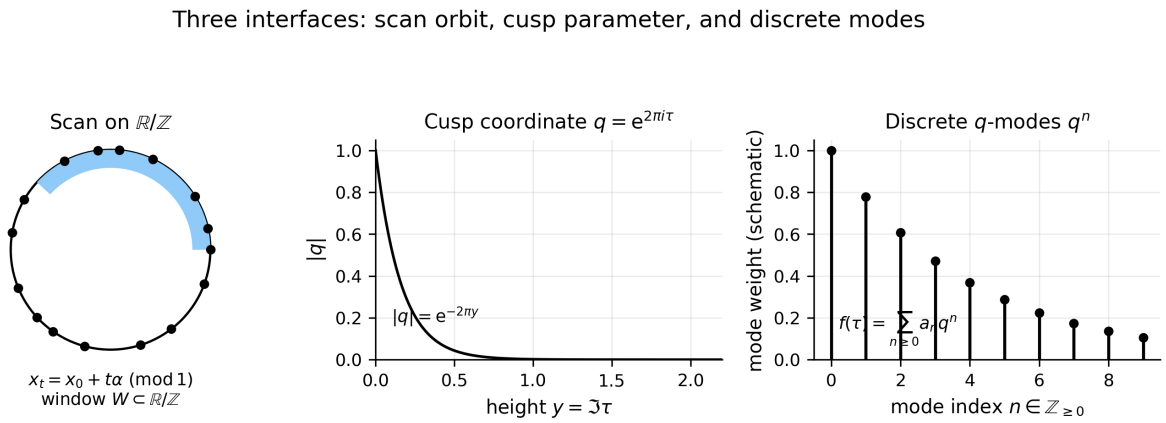

Figure 1: A schematic view of the constitution chain: scan closure on the rotation algebra, an arithmetic-geometric mother space, cusp discretization into coefficients, prime-generated Hecke constraints, and canonical integer-time coding.

Relation to HPA and Ω. We follow the HPA–Ω framework in which the universe is specified by a static global state together with intrinsic automorphisms and holographic/finite-information constraints [1]. We also follow the HPA tool-chain in which unitary scanning, window projection readout, and Ostrowski/Zeckendorf coding form the minimal continuous–discrete bridge [2]. The present paper adds a constitution-level upgrade: it places that scan–projection structure on an explicit arithmetic-geometric mother space (the modular curve) and uses Hecke operators to supply a symmetry-preserving cross-scale skeleton generated by primes.

[1] Interpretation-layer epigraph. The technical content of this paper is stratified (Section 2); metaphors do not enter the Layer 0/1 closure.

Self-containedness (for audit and review). The Layer 0/1 logic of this manuscript is self-contained: all definitions, protocol structures, and quantitative bounds used in the closure chain are stated in this paper with citations to standard literature where appropriate. References to companion manuscripts [1–3] provide broader programmatic context, but are not required to follow or verify any of the arguments presented here.

What is new here. Beyond fixing the layering discipline (Section 2), the main new content is a concrete embedding:

- modular geometry provides a canonical "cusp interface" where analytic data becomes discrete q-series data;
- Hecke algebras provide a prime-generated family of commuting symmetry-preserving operators, offering a clean cross-scale structure;
- continued fractions/Ostrowski numeration provide a canonical map from integer time to locally checkable digit strings, with the golden branch degenerating to Zeckendorf/Fibonacci coding.

Main quantitative statements (audit-ready). The constitution produces finite-data consequences with explicit constants once a concrete scan/readout mapping is fixed:

- **Induced probabilities with deterministic finite-N error.** For window readout $s_t = \mathbf{1}_W(x_t)$ along an irrational-rotation scan, Koksma's inequality yields

$$\left| \frac{1}{N} \sum_{t=0}^{N-1} \mathbf{1}_W(x_t) - |W| \right| \leq 2\, D_N^*(P_N),$$

  and for constant-type slopes (bounded continued-fraction digits) an explicit bound is given in (63).
- **Coefficient recovery from scan sampling with a certified budget.** For T-periodic holomorphic $f(\tau) = \sum_{m\geq 0} a_m q^m$, the scan-quadrature estimator (68) satisfies the deterministic bound (69), and Corollary 9.2 provides an explicit constant-type design inequality.
- **Prime-skeleton rigidity as exact internal constraints.** For Hecke eigenforms, coefficient data obeys multiplicativity and prime-power recursions (Section 9.4); finitely many coefficients determine a form via Sturm bounds (Section 9.4).
- **Protocol identification / fitting templates without simulation.** Appendix C records deterministic fitting and falsification templates (Sturmian/three-gap/Hecke constraints) that can be applied directly to finite readout records with explicit finite-N guarantees.

2 Layering and axioms: a closed argument must be stratified

To prevent "interpretation" from being silently used as "derivation", we make the logic auditable by explicitly separating three layers.

Layer 0 (ontological layer). Only the language of *states and algebras* is allowed. No external time parameter and no external probability postulate is introduced.

Layer 1 (protocol layer). One may choose a scan and readout protocol under finite-resolution constraints. Operational time and statistics are defined *within* the protocol.

Layer 2 (interpretation layer). One maps Layer 1 structures to semantic narratives (spacetime, particles, gravity, entanglement). This layer must be marked interpretive and may not be used as a premise of the Layer 0/1 argument.

This stratification is consistent with the HPA–Ω manuscripts [1, 2] and is adopted here as a strict audit rule.

Figure 2 summarizes the separation and highlights the one-way dependency: Layer 2 interpretation may annotate, but may not be used as a premise.

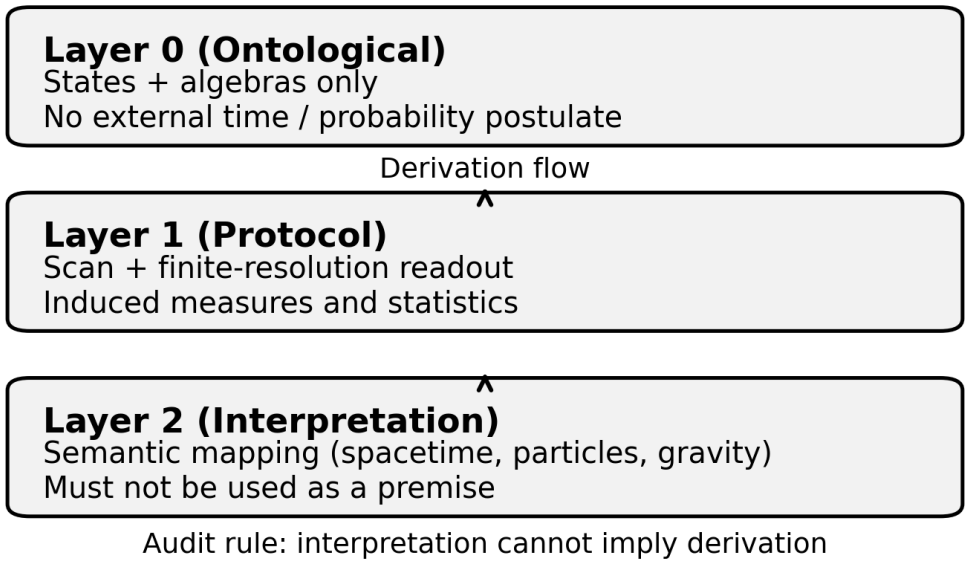

Figure 2: Layer separation and the audit rule. Layer 0 uses only states and algebras; Layer 1 specifies scan and finite-resolution readout protocols and induced measures; Layer 2 provides semantic interpretations and is explicitly excluded from the derivation chain.

2.1 Basic axioms (Omega O1–O4)

Axiom 2.1 (O1 (Omega: static global state))**.** *The universe is specified by a quasi-local operator algebra $\mathcal{A}$ together with a unique normalized global state ω_Ω on $\mathcal{A}$. There is no externally given time-indexed family of states.*

Axiom 2.2 (O2 (finite information))**.** *For any causally closed region, the effective number of degrees of freedom is bounded by a holographic constraint, typically of the form*

$$\dim \mathcal{H}_{\text{region}} \leq \exp\left(\frac{A}{4\ell_P^2}\right), \tag{2}$$

where A is an appropriate boundary area and ℓ_P is the Planck length.

Remark 2.3. *See, e.g., [4] for a standard review of holographic bounds and related formulations of the holographic principle.*

Axiom 2.4 (O3 (causally local discrete update))**.** *There exists a discrete-step automorphism $\mathcal{U} : \mathcal{A} \to \mathcal{A}$ which, in a controlled representation, is implemented by a unitary U and has finite propagation range (a causal locality condition).*

Remark 2.5. *One standard mathematical setting for such discrete-time, locality-preserving updates is quantum cellular automata and related locality-preserving unitary evolutions; see, e.g., [5, 6].*

Axiom 2.6 (O4 (holographic map))**.** *There exists a bulk-to-boundary encoding map Φ which is approximately isometric on an appropriate code subspace and supports observable transport and reconstruction in the sense of algebraic quantum error correction / entanglement wedge reconstruction.*

Remark 2.7. *For standard constructions and results connecting holography, bulk reconstruction, and quantum error correction, see, e.g., [7–9].*

2.2 Upgraded axioms: scan–projection readout and Weyl pairs (O5–O6)

Axiom 2.8 (O5 (scan–projection readout and induced measures))**.** *Finite observers obtain "time" and "probability" from a finite-resolution scan and projection readout of intrinsic phase data. There exists a pointer phase $x \in \mathbb{R}/\mathbb{Z}$ whose scan orbit is sampled at integer ticks $t \in \mathbb{Z}_{\geq 0}$ by*

$$x_t = x_0 + t\alpha \pmod 1, \qquad \alpha \notin \mathbb{Q}. \tag{3}$$

Finite-resolution readout is described by a family of effects $\{E_k^{(\varepsilon)}\}$ (resolution parameter ε) inducing probabilities

$$P_k^{(\varepsilon)} = \omega_{\mathrm{eff}}\left(E_k^{(\varepsilon)}\right), \qquad \sum_k E_k^{(\varepsilon)} = \mathbf{1}, \tag{4}$$

where ω_{eff} denotes the effective state in the observer sector.

Remark 2.9 (standard measurement-theory interface)**.** *The family $\{E_k^{(\varepsilon)}\}$ is a POVM in the usual sense (effects summing to the identity), and $E \mapsto \omega_{\mathrm{eff}}(E)$ is a state on the corresponding effect algebra; see [10, 11] for standard measurement-theory foundations. In finite-dimensional Hilbert-space settings, Gleason-type theorems constrain such probability assignments and justify the Born form under standard assumptions; see [12, 13] for classical statements and extensions.*

In algebraic formulations, one may take ω_{eff} as the restriction of the global state ω_Ω to an observer-accessible subalgebra (or via a conditional expectation onto such a subalgebra), which recovers the familiar reduced-state/partial-trace picture when a tensor-factorization is available; see [14, 15].

Remark 2.10 (continuum parameters versus finite information)**.** *Although O5 models $x \in \mathbb{R}/\mathbb{Z}$ and $\alpha \notin \mathbb{Q}$ as continuum-valued parameters, the framework does not assume that an observer can access their infinite precision. Operationally, access is only through finite-resolution effects $\{E_k^{(\varepsilon)}\}$, and O2 imposes a finite effective information bound. Continuum phase variables should therefore be read as ideal coordinates for a protocol limit, not as physically available infinite storage.*

Axiom 2.11 (O6 (unitary scan algebra: a Weyl pair))**.** *On an effective observer Hilbert space $\mathcal{H}_{\mathrm{eff}}$, there exist a scan unitary U_{scan} and a conjugate phase unitary V satisfying the Weyl relation*

$$U_{\mathrm{scan}} V = \mathrm{e}^{2\pi \mathrm{i}\alpha} V U_{\mathrm{scan}}. \tag{5}$$

A canonical covariant model is given on $L^2(\mathbb{R}/\mathbb{Z})$ by

$$(U_{\mathrm{scan}}\psi)(x) = \psi(x+\alpha), \qquad (V\psi)(x) = \mathrm{e}^{2\pi \mathrm{i} x}\psi(x). \tag{6}$$

Assumption 2.12 (R1 (orbit regularization / finite part))**.** *Regulated-to-continuum passages along scan orbits are fixed by a canonical regularization convention: "Abel first, then limit", which selects a unique finite part for orbit traces and related divergent sums.*

Remark 2.13. *The Abel-regularization convention is a standard summability prescription: one introduces an Abel damping parameter (e.g. r^t with $0 < r < 1$), performs the relevant summation at fixed r, and then takes $r \uparrow 1$ to select a canonical finite part when it exists. See [16] for classical background on Abel summability and related regularization methods.*

Remark 2.14. *Appendix B.16 records an explicit Abel-mean lemma for the irrational-rotation orbit of O5, together with a concrete "finite part" formula on trigonometric polynomials.*

Remark 2.15 (resolvent/Poisson-kernel viewpoint and a finite-coherence motivation)**.** *At the operator level, Abel damping is the canonical resolvent regularization of a unitary scan: for* $|r| < 1$ *one has the convergent geometric series*

$$\sum_{t\geq 0} r^t\, U_{\mathrm{scan}}^t = (1 - r\, U_{\mathrm{scan}})^{-1}, \tag{7}$$

so the Abel-weighted mean $(1-r)\sum_{t\geq 0} r^t(\cdot)$ *corresponds to the standard resolvent-based way of extracting the "DC" (invariant) component while suppressing transient oscillatory modes. On the circle, the same mechanism is the classical Abel/Poisson kernel that recovers boundary data as* $r \uparrow 1$*.*

Protocol-wise, the exponential kernel r^t *may be read as a minimal causal finite-memory response (a discrete first-order low-pass filter): finite observers effectively weight the recent scan history more strongly than the remote past. The idealized protocol limit* $r \uparrow 1$ *corresponds to sending the coherence/memory time to infinity. Other regularizations are possible, but Abel summation is singled out by analyticity and positivity features together with its compatibility with translation symmetry.*

The purpose of O5–O6 is to push "probability" and "measurement" down from Layer 2 to Layer 1: probabilities are induced by finite-resolution effects rather than postulated as external sampling semantics.

3 The arithmetic-geometric stage: the modular curve, hyperbolic fundamental domain, and cusps

This paper's key structural move is to place the minimal scan model of Section 2.2 on an arithmetic-geometric mother space: the modular curve $X(1)$. This section fixes standard definitions and the single geometric fact we will repeatedly exploit: *cusps are identified in the modular quotient, producing a canonical endpoint equivalence.*

3.1 Why $X(1)$: a minimal selection principle and alternatives

The constitution does not claim that $X(1)$ is the only possible mother space. Rather, we adopt the following *minimal selection principle*: among candidate quotients supporting a cusp expansion interface and a large discrete symmetry group, prefer the choice that introduces the least auxiliary structure while keeping the continuous–discrete bridge canonical and auditable.

Selection criteria. The choice $X(1) = \mathrm{PSL}_2(\mathbb{Z})\backslash(\mathbb{H}\cup\{\text{cusps}\})$ is singled out by a conjunction of standard minimality properties:

- **Single cusp and canonical local parameter.** $X(1)$ has a single cusp class and cusp width 1, so the local parameter is the canonical

  $$q = \mathrm{e}^{2\pi \mathrm{i}\tau}, \tag{8}$$

  without additional scaling conventions. This matters constitutionally: the integer Fourier index in a q-series is forced by $T : \tau \mapsto \tau + 1$ and does not depend on a chosen width normalization.

- **Maximal arithmetic symmetry at minimal level.** Level 1 corresponds to the full modular group $\mathrm{PSL}_2(\mathbb{Z})$, i.e. the largest discrete symmetry group in the standard congruence tower. This provides the simplest arena in which cusp q-expansions, modular invariance, and prime-indexed Hecke structure coexist with minimal bookkeeping.

- **Canonical distinguished modular objects.** At level 1 there are canonical generators and invariants (e.g. E_4, E_6, Δ, j) whose q-expansions carry rigid arithmetic structure. This supports the paper's core methodological stance: discreteness is introduced through a standard cusp interface rather than through an ad hoc discretization rule.
- **Canonical dynamics-to-coding bridge.** The geodesic flow on the modular surface admits a classical cross-section coding by continued fractions (Section 4.4). This provides a non-arbitrary origin for the continued-fraction/Ostrowski module used later.

What is not claimed. We do not claim that the above criteria force $X(1)$ uniquely. They justify $X(1)$ as a *minimal* and *canonical* stage on which the scan–projection protocol can be embedded and audited with minimal extra parameters.

Alternatives and generalizations. Several natural alternatives may support a constitution with similar architecture:

- **Other congruence quotients.** Replacing $\mathrm{PSL}_2(\mathbb{Z})$ by a congruence subgroup yields modular curves $X_0(N), X_1(N), X(N)$ with multiple cusps and nontrivial cusp widths. Such choices introduce additional level data and normalization conventions, but may be appropriate if physical sectors are hypothesized to carry level/character structure.
- **Higher-rank automorphic quotients.** More general arithmetic locally symmetric spaces (e.g. higher-rank groups and their Hecke algebras) could provide richer cross-scale operator families. This would require a corresponding upgrade of the scan embedding and the readout interface.
- **Non-arithmetic chaotic stages.** One may attempt to build an analogous constitution on non-arithmetic Anosov systems or other chaotic flows. Such choices can reproduce strong ergodic features but generally lose the prime-indexed rigidity that is central to the present proposal.

In all cases, the audit rule remains: any additional semantic physicalization belongs to Layer 2 and must not be used as a premise of the Layer 0/1 closure.

3.2 The upper half-plane and negative curvature

Let

$$\mathbb{H} = \{\tau \in \mathbb{C} : \Im\tau > 0\} \tag{9}$$

be the Poincaré upper half-plane equipped with the hyperbolic metric

$$\mathrm{d}s^2 = \frac{\mathrm{d}\tau\,\mathrm{d}\overline{\tau}}{(\Im\tau)^2}. \tag{10}$$

One reason hyperbolic geometry is a natural stage under holographic constraints is the exponential growth of boundary "capacity" with hyperbolic radius. While O2 does not uniquely force hyperbolic geometry, the combination "maximal boundary encoding efficiency + strong discrete symmetry" makes $\mathbb{H}$ a canonical candidate arena. Concretely, in curvature -1 one has for the hyperbolic disk B_R of radius R the explicit formulas

$$\mathrm{Area}(B_R) = 4\pi \sinh^2\!\left(\frac{R}{2}\right), \qquad \mathrm{Length}(\partial B_R) = 2\pi \sinh R, \tag{11}$$

so both boundary length and enclosed area grow essentially like e^R as $R \to \infty$ [17]. For background on hyperbolic dynamics on negatively curved surfaces, see [18].

3.3 The modular group, fundamental domain, and cusps

The modular group $\mathrm{PSL}_2(\mathbb{Z})$ acts on $\mathbb{H}$ by fractional linear transformations:

$$\tau \mapsto \gamma \cdot \tau = \frac{a\tau + b}{c\tau + d}, \qquad \gamma = \begin{pmatrix} a & b \\ c & d \end{pmatrix} \in \mathrm{PSL}_2(\mathbb{Z}). \tag{12}$$

It is generated by

$$T : \tau \mapsto \tau + 1, \qquad S : \tau \mapsto -\frac{1}{\tau}. \tag{13}$$

The standard fundamental domain $\mathcal{F} \subset \mathbb{H}$ is bounded by $|\tau| = 1$ and $\Re\tau = \pm\frac{1}{2}$, with the "infinite end" corresponding to the cusp $\tau = \mathrm{i}\infty$.

Figure 3 sketches the standard fundamental domain (truncated at finite height) used throughout.

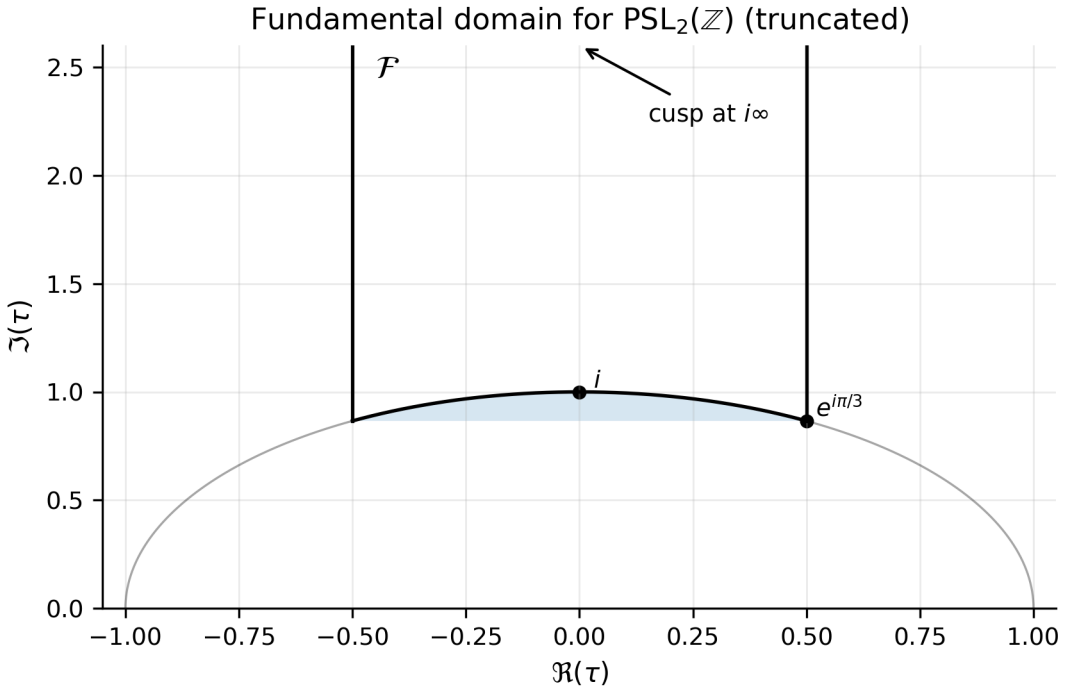

Figure 3: A truncated sketch of the standard fundamental domain $\mathcal{F} \subset \mathbb{H}$ for the action of $\mathrm{PSL}_2(\mathbb{Z})$, bounded by $\Re\tau = \pm\frac{1}{2}$ and $|\tau| = 1$, with the cusp direction $\Im\tau \to \infty$.

Quantitatively, $\mathrm{PSL}_2(\mathbb{Z})\backslash\mathbb{H}$ has finite hyperbolic area. One convenient computation uses Gauss–Bonnet for the orbifold $\mathrm{PSL}_2(\mathbb{Z})\backslash\mathbb{H}$, which has genus $g = 0$, one cusp ($c = 1$), and elliptic points of orders $m_1 = 2$ and $m_2 = 3$. Its orbifold Euler characteristic is

$$\chi_{\mathrm{orb}} = 2 - 2g - c - \sum_i \left(1 - \frac{1}{m_i}\right) = 2 - 0 - 1 - \left(1 - \frac{1}{2}\right) - \left(1 - \frac{1}{3}\right) = -\frac{1}{6}, \tag{14}$$

and for curvature -1 one has $\mathrm{Area} = -2\pi\,\chi_{\mathrm{orb}}$, hence

$$\mathrm{Area}\big(\mathrm{PSL}_2(\mathbb{Z})\backslash\mathbb{H}\big) = \frac{\pi}{3}. \tag{15}$$

See, e.g., [17, 19, 20].

By adjoining the cusps and taking the quotient, one obtains the modular curve

$$X(1) = \mathrm{PSL}_2(\mathbb{Z})\backslash\left(\mathbb{H} \cup \{\text{cusps}\}\right). \tag{16}$$

There is a single cusp on $X(1)$: in the quotient, 0 and ∞ lie in the same $\mathrm{PSL}_2(\mathbb{Z})$-orbit (indeed, S exchanges 0 and ∞), so they define the same cusp class.

Remark 3.1 (interpretation-layer hint: UV/IR endpoint identification)**.** *The identification $0 \sim \infty$ is an arithmetic-topological statement about the modular quotient. Any physical reading—for example, interpreting S as a scale inversion template—belongs to Layer 2 and is not used as a premise.*

Remark 3.2 (interpretation-layer template: the cusp as an "observer singularity")**.** *On $X(1)$ there is a single cusp class, and it is precisely where the canonical local parameter $q = \mathrm{e}^{2\pi \mathrm{i} \tau}$ is defined and where q-expansions are anchored. In a holographic reading, one may regard the cusp as a "light source" for projection: continuous scan data becomes accessible as discrete coefficient data through the cusp q-expansion interface. This is a Layer 2 metaphor and is not used as a premise.*

Remark 3.3 (interpretation-layer metaphor: a prism vocabulary)**.** *In a prism vocabulary, the single cusp class plays the role of a "source point" where an undifferentiated continuous object is presented to the readout interface, while the cusp q-expansion disperses that object into a discrete "spectrum" of coefficient labels. This is a Layer 2 semantic picture attached to the mathematical fact that q is the canonical local parameter at the cusp; it is not used as a premise.*

4 Scanning as modular flow: from rotation algebras to modular dynamics

This section explains how the scan algebra (O6) can be viewed as a minimal cross-section of modular dynamics. The main point is structural: the Weyl relation singles out the irrational rotation algebra (a noncommutative torus), while the modular generators S, T provide canonical geometric symmetries whose cusp action supplies a scale-inversion template.

4.1 The rotation algebra A_α as the minimal scan closure

The C^*-algebra generated by unitaries U, V satisfying

$$UV = \mathrm{e}^{2\pi \mathrm{i} \alpha} VU, \qquad \alpha \notin \mathbb{Q}, \tag{17}$$

is the (irrational) rotation algebra A_α [21, 22]. In the scan interpretation:

- U encodes the tick iteration (time as an integer counter),
- V encodes the phase/readout coordinate.

This is the smallest closed algebraic setting in which scanning and phase readout coexist while remaining intrinsically noncommutative.

Related structures: noncommutative tori, Diophantine constraints, and elliptic/modular bridges. The identification of the scan algebra with a noncommutative torus is not merely terminological: the rotation algebra supports a rich "geometric" apparatus (modules, vector bundles, Chern numbers) and exhibits Diophantine rigidity phenomena closely related to TKNN-type constraints in quantum Hall settings [23]. Moreover, there are explicit bridges between modules over noncommutative tori and elliptic-curve geometry [24], which provides additional context for why it is natural to interface the scan algebra with modular/elliptic backgrounds in the present constitution.

4.2 T-translation and phase periodicity

On $\mathbb{H}$, the modular translation $T : \tau \mapsto \tau + 1$ induces

$$q = \mathrm{e}^{2\pi \mathrm{i}\tau} \mapsto \mathrm{e}^{2\pi \mathrm{i}(\tau+1)} = q, \tag{18}$$

so the q-coordinate is T-periodic. At the same time, the real part shifts by an integer:

$$x := \Re\tau \pmod 1 \quad \Rightarrow \quad x \mapsto x + 1 \equiv x. \tag{19}$$

This identifies a canonical boundary phase coordinate $x \in \mathbb{R}/\mathbb{Z}$ compatible with modular periodicity. The scan orbit of O5,

$$x_t = x_0 + t\alpha \pmod 1, \tag{20}$$

is then an irrational translation on the same circle: it respects the same quotient structure but selects an irrational slope (minimality and unique ergodicity are standard; see e.g. [18, 25]). By Weyl's equidistribution theorem, the orbit is equidistributed on $\mathbb{R}/\mathbb{Z}$ and thus induces the Lebesgue measure at the readout level.

The roles of α and τ are coordinated but not identical. The parameter α is the scan slope in the Weyl pair (O6): it controls the boundary rotation $x \mapsto x + \alpha$ and therefore the deterministic sampling law of the phase circle. The modular coordinate $\tau \in \mathbb{H}$ plays a different role: it is the geometric coordinate on the mother space and carries an additional scale parameter $y = \Im\tau$. The constitution couples them by a *choice of embedding* of the boundary scan into the modular stage, e.g. along a horizontal line

$$\tau_t := x_t + \mathrm{i}y, \tag{21}$$

as used in Section 9.6 and in the coefficient recovery bounds of Section 9.3. There is no claim of a canonical identification $\alpha \leftrightarrow \tau$ beyond such protocol choices: α determines the scan sampling on x, while τ (and in particular y) parametrizes the cusp interface and numerical stability of q-expansions. The continued-fraction/Gauss-map coding arises instead from a different dynamical object (modular geodesic flow; Section 4.4) and should not be conflated with the scan slope.

4.3 S-inversion, cusp equivalence, and a scale-exchange template

The modular inversion $S : \tau \mapsto -1/\tau$ exchanges deep and shallow regions of the cusp. Indeed, if $\Im\tau$ is large (near $\mathrm{i}\infty$), then $\Im(-1/\tau)$ is small (near 0). Since $0 \sim \infty$ as cusps on $X(1)$ (Section 3.3), S supplies a canonical endpoint identification on the arithmetic quotient.

Remark 4.1 (interpretation-layer template: "semantic wormhole")**.** *Mathematically, S is an involution that exchanges deep and shallow cusp regions and realizes an endpoint identification in the modular quotient. In an HPA–Ω interpretation, this can be used as a template for a non-local* semantic wormhole*: a symmetry channel that relates coarse (IR) and fine (UV) descriptions without traversing all intermediate scan ticks in a naive linear parametrization. This language is interpretive (Layer 2) and is not required for the Layer 0/1 closure.*

4.4 Geodesic flow on the modular surface and continued fractions

A key bridge in this constitution is that *continued fractions are not an arbitrary coding choice*: they arise canonically from the dynamics of the modular surface. Let

$$M := \mathrm{PSL}_2(\mathbb{Z})\backslash\mathbb{H} \tag{22}$$

be the modular surface (an orbifold of finite hyperbolic area). The geodesic flow on M admits a classical symbolic coding in which the digit sequence of a continued fraction is the itinerary of a geodesic with respect to a natural cross-section. Concretely, the Gauss map

$$G(\xi) = \left\{ \frac{1}{\xi} \right\}, \qquad \xi \in (0,1), \tag{23}$$

is the base map of a standard suspension model for the modular geodesic flow [18, 26].

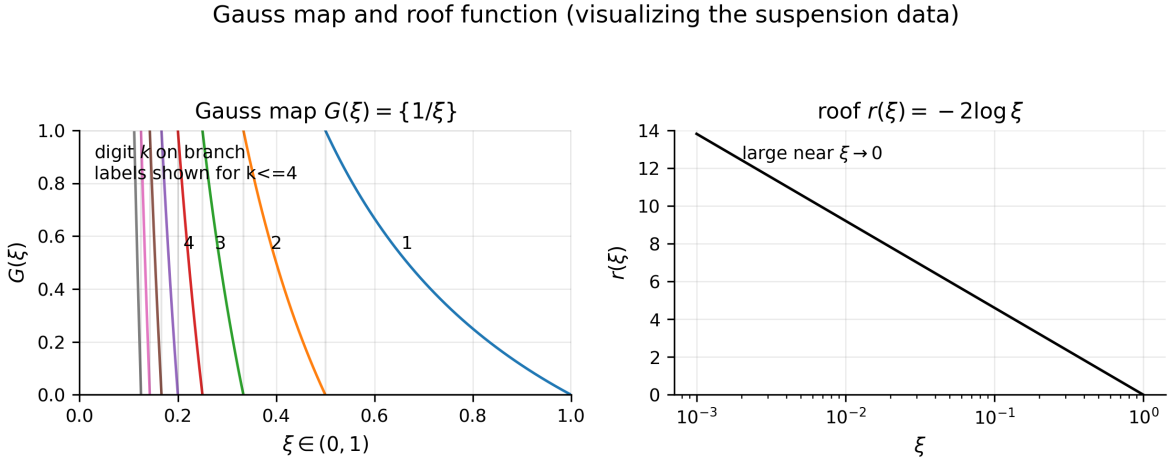

Figure 4: A schematic bridge (Series) between the modular geodesic flow and the Gauss-map suspension: continued-fraction digits arise canonically as return symbols on a cross-section, with a roof function controlling return times.

Theorem 4.2 (Series: modular geodesic flow as a suspension over the Gauss map)**.** *There exists a Poincaré cross-section $\Sigma \subset T^1M$ for the geodesic flow and a measurable identification of Σ with $(0,1)$ such that the first-return map on Σ is (conjugate to) the Gauss map G. Moreover, the geodesic flow on M is measurably isomorphic to the suspension flow over G with roof function*

$$r(\xi) = -2\log\xi. \tag{24}$$

In particular, the continued-fraction digits of $\xi = [0; a_1, a_2, \ldots]$ arise as the symbolic itinerary of the corresponding modular geodesic under successive returns.

Theorem 4.3 (Gauss measure and digit law)**.** *The Gauss map $G(\xi) = \{1/\xi\}$ preserves the probability measure*

$$\mathrm{d}\mu(\xi) = \frac{1}{\log 2}\,\frac{\mathrm{d}\xi}{1+\xi}, \qquad \xi \in (0,1), \tag{25}$$

and is ergodic with respect to μ [27]. Writing $\xi = [0; a_1, a_2, \ldots]$, the first digit satisfies

$$\mu(a_1 = k) = \log_2\!\left(1 + \frac{1}{k(k+2)}\right) \qquad (k \geq 1). \tag{26}$$

In particular, for μ-almost every ξ the digit frequencies along the orbit are governed by this law (Birkhoff theorem).

Theorem 4.4 (Gauss–Kuzmin exponential convergence (classical))**.** *Let ν be a probability measure on $(0,1)$ that is absolutely continuous with respect to Lebesgue measure with a density of bounded variation. Then there exist constants $C > 0$ and $0 < \rho < 1$ such that for all $n \geq 0$,*

$$\sup_{x \in (0,1)} |\nu(G^n(\xi) \leq x) - \mu((0,x])| \leq C\,\rho^n, \tag{27}$$

where μ is the Gauss invariant measure from Theorem 4.3 (so $\mu((0,x]) = \log_2(1+x)$). Equivalently, digit statistics relax exponentially fast to the Gauss digit law along typical continued-fraction tails. The optimal ρ is known as the Gauss–Kuzmin–Wirsing constant, numerically $\rho \approx 0.30366$; see [27].

Remark 4.5 (quantitative relaxation-to-equilibrium)**.** *Theorem 4.4 upgrades the digit law from an "almost-everywhere" statement to a* finite-time *relaxation guarantee for a broad class of initial distributions.*

Remark 4.6 (constitution-level consequence)**.** *This modular-geodesic origin provides a strict mother-space justification for the continued-fraction/Ostrowski module used in Section 7: the digits $\{a_n\}$ are canonical dynamical invariants of modular geodesics, and Ostrowski numeration is the corresponding canonical integer-time coordinate system.*

4.5 Boundary irrationals as geodesic endpoints: a canonical meaning of the continued fraction of α

The coordinate $\xi \in (0,1)$ in the Gauss-map suspension description (Theorem 4.2) is not an auxiliary "coding parameter": it is naturally a boundary coordinate. Indeed, the boundary at infinity of $\mathbb{H}$ is $\partial\mathbb{H} = \mathbb{R} \cup \{\infty\} \cong \mathbb{P}^1(\mathbb{R})$, and every (unoriented) geodesic in $\mathbb{H}$ is uniquely determined by its unordered pair of endpoints in $\partial\mathbb{H}$. After quotienting by $\mathrm{PSL}_2(\mathbb{Z})$, the geodesic flow on $M = \mathrm{PSL}_2(\mathbb{Z})\backslash\mathbb{H}$ inherits a canonical cross-section whose return dynamics is described by the Gauss map on such boundary coordinates [18, 26].

Why this matters for scan slopes. The scan slope α in O5/O6 is a boundary irrational parameter: $\alpha \in \mathbb{R}/\mathbb{Z}$ can be represented by a unique $\alpha \in (0,1) \setminus \mathbb{Q}$ after choosing a lift. Thus, once a scan slope α is fixed, its continued-fraction digits are canonically meaningful from the mother-space viewpoint: they coincide with the symbolic return itinerary of the modular geodesic associated to the boundary coordinate $\xi = \alpha$ in the Series cross-section picture. This does *not* identify the scan orbit $x_t = x_0 + t\alpha$ with geodesic flow; it clarifies that the Ostrowski numeration system built from the continued fraction of α (Section 7.2) is a modular-dynamical invariant attached to the same boundary irrational parameter that controls the scan.

Constitution-level consequence. The coding module (continued fractions/Ostrowski/Zeckendorf) is therefore not an ad hoc digitization of α: once the modular stage is adopted, it is the canonical arithmetic coding naturally associated with the boundary irrational that parametrizes the scan.

5 Readout as a q-expansion: from continuous data to discrete integers

The bridge from continuous analytic data to discrete arithmetic data is canonically realized at a cusp via Fourier/q-expansion. This section formalizes the slogan "discreteness lives at cusps" as a protocol-level interface: cusp expansions provide a standard, symmetry-compatible discretization map.

5.1 Modular forms and cusp expansions

Let f be a modular form of weight k for $\mathrm{PSL}_2(\mathbb{Z})$ (or a congruence subgroup). At the cusp ∞, one has a q-expansion

$$f(\tau) = \sum_{n \geq 0} a_n q^n, \qquad q = \mathrm{e}^{2\pi \mathrm{i} \tau}. \tag{28}$$

For a cusp form, $a_0 = 0$. Many arithmetic objects have integral (or algebraic-integer) coefficients a_n. A central example is the discriminant modular form

$$\Delta(q) = q \prod_{n\geq 1} (1-q^n)^{24} = \sum_{n\geq 1} \tau(n) q^n, \tag{29}$$

whose coefficients $\tau(n)$ are the Ramanujan tau function. Standard references for modular forms, q-expansions, and the arithmetic nature of Fourier coefficients include [19, 20, 28].

Proposition 5.1 (discreteness from T-periodicity at the cusp)**.** *Let f be holomorphic on $\mathbb{H}$ and T-periodic: $f(\tau+1) = f(\tau)$. Writing $\tau = x + \mathrm{i}y$, the function $x \mapsto f(x+\mathrm{i}y)$ is 1-periodic for every fixed $y > 0$ and therefore admits a Fourier expansion*

$$f(x+\mathrm{i}y) = \sum_{n\in\mathbb{Z}} a_n(y)\, \mathrm{e}^{2\pi \mathrm{i} n x}, \qquad a_n(y) = \int_0^1 f(x+\mathrm{i}y)\, \mathrm{e}^{-2\pi \mathrm{i} n x}\, \mathrm{d}x. \tag{30}$$

If, in addition, f has at most polynomial growth as $y \to \infty$ (the standard cusp-growth condition satisfied by modular forms), then $a_n(y) = 0$ for all $n < 0$, and the nonnegative modes can be written as a q-series

$$f(\tau) = \sum_{n\geq 0} a_n\, q^n, \qquad q = \mathrm{e}^{2\pi \mathrm{i}\tau}, \tag{31}$$

with a_n independent of y.

Remark 5.2. *This proposition makes the constitution-level point precise:* the integer mode index is forced by the T-quotient. *The cusp parameter q is simply the holomorphic packaging of the Fourier modes. See standard treatments in [19, 20].*

Protocol-level reading. If τ is treated as a scan coordinate, then the monomials q^n serve as canonical "cusp modes", and the q-expansion maps a continuous analytic object to a discrete coefficient sequence $\{a_n\}$. In finite-resolution readout, one naturally accesses only a truncated or windowed subset of these modes; this aligns with O5, where probabilities are induced by finite-resolution effects rather than externally postulated sampling rules.

Generative versus retrieval (interpretation-layer viewpoint). One may additionally emphasize a *generative* perspective: the discrete sequence $\{a_n\}$ is not treated as "downloaded" from a static database, but as *rendered* by a scan–projection procedure applied to a generating object f at a cusp. This is a Layer 2 viewpoint about the semantics of readout and does not alter the Layer 0/1 mathematical content.

Remark 5.3 (interpretation-layer metaphor: dispersion into coefficients)**.** *In the same semantic vocabulary, one may view the cusp interface as a "prism": an undifferentiated generating object f is dispersed into discrete coefficient labels $\{a_n\}$ by the q-expansion, and finite-resolution readout corresponds to accessing only a band-limited or truncated portion of that spectrum. This is a Layer 2 metaphor and is not used as a premise.*

Remark 5.4 (what is and is not claimed)**.** *We do* not *claim as a theorem that physical particle spectra must equal $\{a_n\}$. The only constitution-level claim is that cusp expansions provide a clean, auditable discretization interface: if a physical readout is dominated by cusp Fourier modes, then the discrete output inherits arithmetic structure.*

5.2 Ramanujan's differential system: a canonical q-flow on modular data

The cusp parameter $q = \mathrm{e}^{2\pi \mathrm{i}\tau}$ provides not only an expansion interface but also a canonical derivation

$$D := q\frac{\mathrm{d}}{\mathrm{d}q} = \frac{1}{2\pi \mathrm{i}}\frac{\mathrm{d}}{\mathrm{d}\tau}, \tag{32}$$

which differentiates along the cusp coordinate. For level 1, the differential closure of modular forms is controlled by the weight-2 Eisenstein series

$$E_2(\tau) = 1 - 24\sum_{n\geq 1}\sigma_1(n)\, q^n, \tag{33}$$

which is *quasi*-modular rather than modular. The classical Ramanujan identities state that

$$DE_2 = \frac{E_2^2 - E_4}{12}, \qquad DE_4 = \frac{E_2E_4 - E_6}{3}, \qquad DE_6 = \frac{E_2E_6 - E_4^2}{2}, \tag{34}$$

and, equivalently, the logarithmic derivative of the discriminant satisfies

$$D\log\Delta = E_2. \tag{35}$$

These identities are standard and can be found in classical references such as [19, 20].

Constitution-level role. Equations (34)–(35) make explicit that the cusp interface comes with a rigid differential calculus: once q is adopted as the canonical local coordinate, modular data is organized not only by discrete coefficients but also by a canonical q-flow (the Ramanujan vector field). In the present constitution this provides an arithmetic-dynamical meaning to the slogan "viewed from the cusp": the same canonical coordinate that produces discrete q-coefficients also supports a closed differential system relating the distinguished generators E_4, E_6, Δ.

5.3 Modular symbols and periods: critical L-values as period data

The q-expansion interface produces discrete coefficients. A complementary, equally standard interface produces *period data* from modular forms: integrals of modular differentials along rational paths on the modular curve (modular symbols). These integrals are periods in the sense of Kontsevich–Zagier [29] and, from the motivic viewpoint, encode comparison data between Betti and de Rham realizations.

Modular symbols (period integrals). Let f be a cusp form of weight $k \geq 2$ for a congruence subgroup (in particular for $\mathrm{SL}_2(\mathbb{Z})$). For integers m with $1 \leq m \leq k-1$ and for cusps/rational endpoints $r, s \in \mathbb{Q}\cup\{\infty\}$, one considers integrals of the form

$$\{r, s\}_f^{(m)} := \int_r^s f(z)\, z^{m-1}\, \mathrm{d}z, \tag{36}$$

where the path is taken in $\mathbb{H}$ and endpoints are interpreted as cusps. These modular symbol values generate a finite-dimensional period lattice attached to f; see standard accounts in [28, 30, 31].

Mellin transform and L-values. The Dirichlet series

$$L(f, s) := \sum_{n\geq 1}\frac{a_n}{n^s} \tag{37}$$

admits the classical Mellin transform representation (for $\Re(s)$ large, with analytic continuation thereafter):

$$(2\pi)^{-s}\Gamma(s)\,L(f,s) = \int_0^\infty f(\mathrm{i}t)\,t^{s-1}\,\mathrm{d}t. \tag{38}$$

In particular, critical values $L(f,m)$ for integers $1 \le m \le k-1$ can be expressed in terms of the period data generated by (36); see [30–32].

Algebraicity after period normalization (standard theorem). For a normalized Hecke eigen cusp form f with coefficient field K_f, there exist nonzero periods $\Omega_f^{\pm}$ (depending on f but not on m) such that for each critical integer m one has

$$\frac{L(f,m)}{(2\pi\mathrm{i})^m\,\Omega_f^{\pm}} \in K_f, \tag{39}$$

with the choice of sign determined by the parity dictated by complex conjugation (see [30, 32]). This is the precise sense in which critical L-values are periods up to algebraic factors.

Constitution-level role. Equation (39) provides a *period interface* parallel to the q-expansion interface: it converts the same underlying modular object into numeric invariants that are stable under changes of realization. In the broader HPA–Ω program, MAI ([3]) supplies a protocol-level period-realization interface for scan averages, and the remaining objective is to align that interface with modular period data and with the Hecke/Frobenius invariants on the étale side.

5.4 Induced measures: probability from window kernels

O5 states that finite-resolution readout is encoded by effects $\{E_k^{(\varepsilon)}\}$, yielding

$$P_k^{(\varepsilon)} = \omega_{\mathrm{eff}}\left(E_k^{(\varepsilon)}\right), \qquad \sum_k E_k^{(\varepsilon)} = \mathbf{1}. \tag{40}$$

This has a direct "cusp mode" interpretation: a window kernel can be understood as a finite bandwidth or finite depth in n for which the coefficients a_n are operationally accessible. Probability is then an induced measure built from the spectral data and the window.

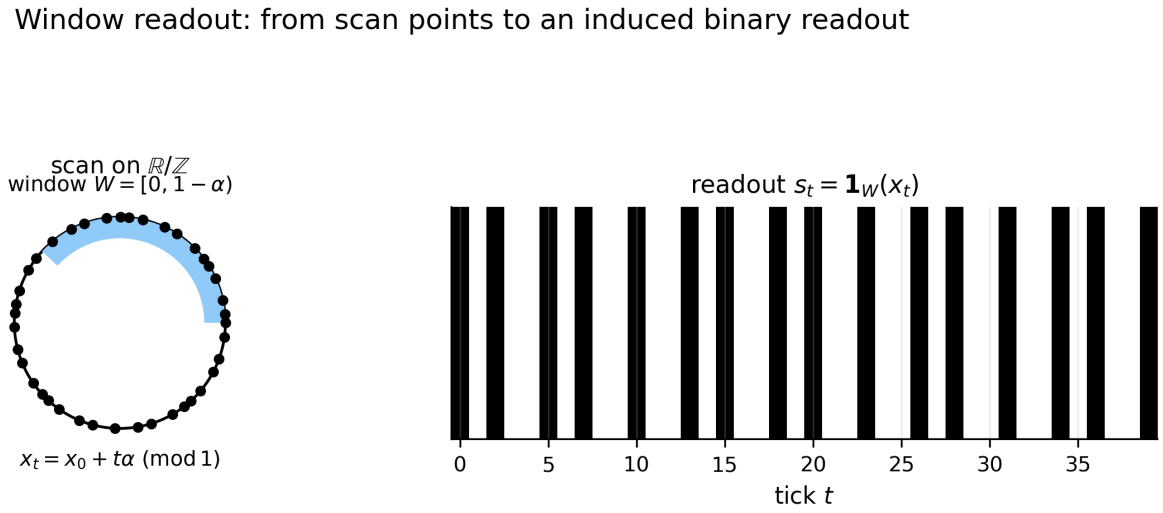

Figure 5: Protocol-level schematic of induced probability: scan dynamics on a phase circle is paired with a finite-resolution instrument (effects/windows), producing induced outcome probabilities by evaluation in an effective state.

6 Hecke dynamics and the prime skeleton: symmetry-preserving cross-scale scanning

The Hecke algebra provides a canonical arithmetic mechanism for "cross-scale" structure: it is a commuting family of symmetry-preserving operators acting on modular forms, generated by primes and governed by rigid multiplicative relations. This section records the standard facts we need and clarifies the precise role of primes.

6.1 Hecke operators and symmetry preservation

Let M_k be a space of modular forms of weight k (for $\mathrm{PSL}_2(\mathbb{Z})$ or a congruence subgroup). For each integer $n \geq 1$, the Hecke operator T_n is a linear endomorphism of M_k preserving modular symmetry. In terms of q-expansions, if

$$f(\tau) = \sum_{m \geq 0} a_m q^m, \tag{41}$$

then

$$(T_n f)(\tau) = \sum_{m \geq 0} \left(\sum_{d \mid (m,n)} d^{k-1}\, a_{mn/d^2} \right) q^m. \tag{42}$$

Hecke operators commute on appropriate subspaces and can be simultaneously diagonalized [20, 28].

6.2 Why primes: generators rather than exclusive definitions

It is important to state the "prime skeleton" correctly:

- T_n is defined for all positive integers n.
- The Hecke algebra is generated by the operators T_p at primes p.

The key relations are

$$T_m T_n = \sum_{d \mid (m,n)} d^{k-1}\, T_{mn/d^2}, \tag{43}$$

and the prime-power recursion

$$T_{p^{r+1}} = T_p T_{p^r} - p^{k-1} T_{p^{r-1}}. \tag{44}$$

Thus the full family $\{T_n\}$ is built from prime data.

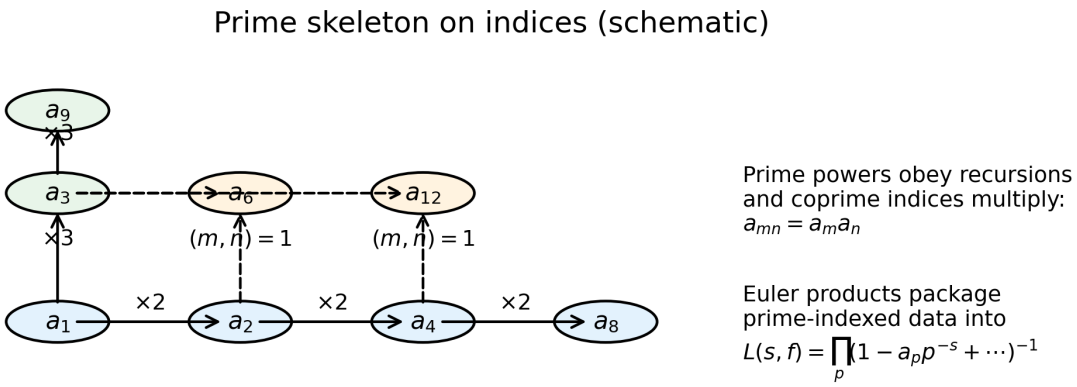

Figure 6: The prime skeleton viewpoint (schematic): prime-indexed generators and Hecke relations constrain the full coefficient spectrum of eigenforms, and package into Euler products with local factors indexed by primes.

6.3 Protocol-level origin: symmetry-preserving coarse-graining and Hecke correspondences

The constitution's use of Hecke operators is not meant as an isolated analogy. At Layer 1, "cross-scale" refers to changing observational resolution while preserving the structural symmetries that define the stage. Once the stage is modular and the discrete interface is anchored at the cusp, there is a canonical family of symmetry-preserving coarse-graining operators: the Hecke correspondences.

Coarse-graining must be symmetry-preserving. In the scan–projection protocol (O5/O6), a change of scale may be realized by a controlled decimation of tick time (subsampling) together with an instrument-induced averaging over micro-shifts that are operationally unresolved. On the modular side, the same idea takes a canonical arithmetic form: one averages over finite-index sublattices (equivalently, over isogeny classes) in a way that commutes with the modular symmetry.

A boundary toy model: decimation with fiber averaging. At the simplest boundary level (the phase circle $x \in \mathbb{R}/\mathbb{Z}$), one may model a symmetry-preserving "coarse" operator by the translation-invariant fiber average over the n-fold covering:

$$(\mathcal{C}_n g)(x) := \frac{1}{n} \sum_{b=0}^{n-1} g\Big(\frac{x+b}{n}\Big). \tag{45}$$

This implements a decimation/averaging step without selecting a preferred micro-shift; it also satisfies $\mathcal{C}_m \mathcal{C}_n = \mathcal{C}_{mn}$ by a direct reindexing of the double sum. The modular Hecke operators can be read as the natural arithmetic lift of this "scale-change + shift-average" motif to the modular stage.

Hecke as an averaging operator over index-n sublattices. For level 1, a standard representative description is the explicit formula

$$(T_n f)(\tau) = n^{k-1} \sum_{\substack{ad=n \\ d>0}} \sum_{b \pmod d} d^{-k} f\Big(\frac{a\tau + b}{d}\Big), \tag{46}$$

which is equivalent to the q-expansion action (42) and can be viewed as averaging over a finite correspondence indexed by determinant n (see Appendix B.15 for the classical formula and references). The determinant constraint $ad = n$ is precisely the discrete scale label: it is the index of the sublattice in the elliptic-curve lattice model, hence a canonical "coarse" scale associated with n.

Decimation and shift-averaging at the cusp. The maps $\tau \mapsto (a\tau + b)/d$ decompose into a scaling component (controlled by a/d) and a discrete translation (indexed by $b (\mathrm{mod}\ d)$). In protocol terms, b-averaging implements a symmetry-preserving micro-shift average compatible with T-periodicity, while the scaling component encodes a discrete resampling/coarse-graining step. The resulting operator is therefore not an arbitrary choice: it is the standard symmetry-compatible way to implement "change of scale" once modular symmetry and the cusp interface have been adopted.

Why primes emerge. Since finite-index data factorizes multiplicatively and the Hecke algebra is generated by the prime-indexed operators T_p, the full cross-scale family propagates from prime steps. This is the technical content behind the "prime skeleton": primes are the canonical generator labels for scale-changing correspondences, not an extra physical postulate.

Related work: Hecke symmetries beyond scalar modular forms. Hecke relations and Hecke-type operators also play a prominent role in physics-adjacent settings where the relevant modular objects are *vector-valued* (e.g. RCFT characters and modular tensor categories), providing additional context and constraints on any "prime skeleton" interpretation. For example, Hecke relations can induce nontrivial Galois symmetries in RCFT/MTC data [33], and there are systematic constructions of Hecke operators acting on vector-valued modular forms [34]. These developments suggest a natural upgrade path for the constitution when readout sectors are modeled by vector-valued modular objects rather than scalar forms.

6.4 Eigenforms and stable discrete spectra

If f is a (normalized) Hecke eigenform, then for all n,

$$T_n f = \lambda_n f, \tag{47}$$

and typically $\lambda_n = a_n$ in the q-expansion normalization. Consequently the coefficients $\{a_n\}$ satisfy rigid arithmetic constraints (multiplicativity on coprime indices and prime-power recursions). In protocol terms: if "repeatable discrete readout" corresponds to stable eigen-structures under symmetry-preserving cross-scale operations, then eigenforms supply a mathematically controlled model of such stability, with primes functioning as the generating skeleton.

Euler product: the prime skeleton in closed form. For a normalized eigenform $f(\tau) = \sum_{n\geq 1} a_n q^n$ (with $a_1 = 1$), the associated Dirichlet series

$$L(f, s) = \sum_{n\geq 1} \frac{a_n}{n^s} \tag{48}$$

admits an Euler product whose local factors are determined by primes:

$$L(f, s) = \prod_p \left(1 - a_p p^{-s} + p^{k-1-2s}\right)^{-1} \qquad \text{(level 1)}, \tag{49}$$

see, e.g., [19, 20, 28]. For the discriminant form Δ of weight 12, this reads

$$\sum_{n\geq 1} \frac{\tau(n)}{n^s} \;=\; \prod_p \left(1 - \tau(p) p^{-s} + p^{11-2s}\right)^{-1}, \tag{50}$$

which makes the "prime-generated skeleton" literal: primes control the local factors and the Hecke relations propagate them to all n.

Remark 6.1 (interpretation-layer metaphor: a prime spectrum)**.** *In a prism vocabulary, the Euler product expresses the idea that "colors" are prime-indexed: primes determine local spectral factors, and the commuting Hecke algebra acts as a symmetry-preserving family of "spectral filters" whose eigenforms are the stable directions (Section 6.4). This language is interpretive (Layer 2) and is not used as a premise.*

Diagonalization is canonical on cusp forms. On spaces of cusp forms equipped with the Petersson inner product, Hecke operators are normal and, in standard settings, self-adjoint. Combined with commutativity, this yields an orthogonal basis of simultaneous Hecke eigenforms (a genuine diagonalization frame). See, e.g., [19, 28] and Appendix B.15.

Remark 6.2 (interpretation-layer metaphor: holographic resonance)**.** *In an interpretation-layer reading, "eigenform stability" may be viewed as a resonance condition: when scan dynamics is aligned with a Hecke-eigen structure, readout becomes exceptionally stable under coarse-graining and finite-resolution noise. Any identification of such resonance with cognitive notions (e.g. "intuition") is semantic and is not used as a premise.*

7 From modular scan geometry to HPA coding: continued fractions, Ostrowski numeration, and Zeckendorf

This section connects the scan orbit of O5 to canonical integer-time coding. The bridge proceeds in three standard steps: irrational rotations yield Sturmian (mechanical) words under window readout; continued fractions yield Ostrowski numeration as a canonical representation of integers; and the golden branch degenerates to Zeckendorf/Fibonacci coding.

7.1 Irrational rotation + window readout yields Sturmian words

Given an irrational rotation orbit

$$x_t = x_0 + t\alpha \pmod 1, \qquad \alpha \notin \mathbb{Q}, \tag{51}$$

choose an interval window $W \subset \mathbb{R}/\mathbb{Z}$ and define a binary readout

$$s_t = \mathbf{1}_W(x_t) \in \{0, 1\}. \tag{52}$$

The resulting infinite word is a Sturmian (mechanical) word and has minimal subword complexity: the number of distinct length-n subwords equals $n + 1$ [35, 36]. This aligns with the HPA emphasis on "binary-minimal" readout grammars. In particular, on the golden branch $\alpha = \varphi^{-1}$ with the canonical window $W = [0, 1 - \alpha)$, the associated mechanical word is the Fibonacci word (a classical fixed point of the substitution $0 \mapsto 01$, $1 \mapsto 0$).

7.2 Ostrowski numeration from continued fractions

Let $\alpha = [0; a_1, a_2, \ldots]$ be the continued fraction of α, and let q_n be the denominators of the convergents. The Ostrowski numeration system represents every integer N uniquely as

$$N = \sum_n b_n q_n, \qquad 0 \le b_n \le a_{n+1}, \tag{53}$$

subject to local admissibility constraints (a finite "no-carry" grammar) determined by the continued fraction. This provides a canonical encoding of integer tick time into a digit string with

local checkability, which is essential under finite-resolution and locality constraints: the readout protocol must be implementable in a quasi-local algebra. Background on Ostrowski numeration and its role in automatic/low-complexity sequences can be found in [37].

Remark 7.1 (metrical scaling constants (standard))**.** *The continued-fraction digits encode more than a convenient grammar: the metrical theory yields sharp typical scaling constants. If p_n/q_n are convergents of α and $\alpha = [0; a_1, a_2, \ldots]$, then for Lebesgue-a.e. α one has the Lévy limit*

$$\lim_{n\to\infty} \frac{1}{n} \log q_n = \frac{\pi^2}{12 \log 2}, \tag{54}$$

and Khinchin's constant for the geometric mean of digits,

$$\lim_{n\to\infty} \left(\prod_{j=1}^{n} a_j \right)^{1/n} = K_0 \approx 2.6854520010, \tag{55}$$

see, e.g., [27]. These constants quantify the "exponential scaling" implicit in the canonical coding.

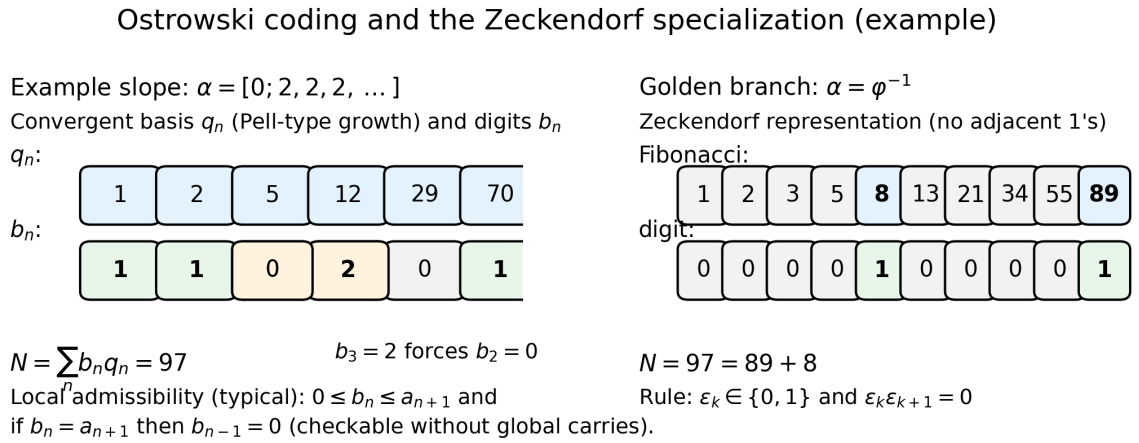

Figure 7: Ostrowski numeration and local admissibility (schematic): integer time is encoded in locally checkable digits in the convergent basis; on the golden branch this specializes to the Zeckendorf rule forbidding adjacent 1's.

7.3 The golden branch and Zeckendorf degeneration

For the golden branch $\alpha = \varphi^{-1} = [0; 1, 1, 1, \ldots]$, all continued-fraction coefficients satisfy $a_n = 1$, and Ostrowski numeration degenerates to Zeckendorf representation:

$$N = \sum_k \epsilon_k F_k, \qquad \epsilon_k \in \{0, 1\}, \qquad \epsilon_k \epsilon_{k+1} = 0, \tag{56}$$

where $\{F_k\}$ are Fibonacci numbers. The single local constraint "no adjacent 1" gives a particularly economical binary code, while retaining strong aperiodicity and good uniform-distribution and discrepancy properties in the associated scan readout [38, 39].

8 Interfaces with Ω theory and QCA micro-models (interpretation layer)

This section is *interpretation-layer* only (Layer 2): it records how the constitution-level chain may be interfaced with micro-dynamical models and physical semantics. None of the statements below are used as premises in the Layer 0/1 closure.

8.1 QCA, quasicrystal textures, and scan–texture unification

In the Ω framework, micro-dynamics may be modeled by causally local quantum cellular automata (QCA) subject to finite-information and holographic constraints. For background on QCA as unitary, locality-preserving discrete-time dynamics, see [5, 6]; for the Ω-specific holographic constraints, see [1]. Sturmian/Fibonacci words arising from golden-branch scanning can serve as quasi-periodic textures for 1D automata and can be embedded into cut-and-project quasicrystal constructions [40], providing a controlled route toward continuum Dirac-like limits in suitable scaling regimes [2, 41].

8.2 Gravity as readout mismatch: phase-pressure templates

In one interpretation-layer extension of HPA–Ω, gravity is modeled as a coarse-grained effect of mismatch between intrinsic unitary scanning and low-dimensional projection readout ("phase pressure"). Turning this into a predictive theory requires additional dynamical closure beyond the constitution presented here.

8.3 Computational teleology and resource semantics

With time defined as scan iteration and space tied to readout resolution, one may interpret complexity as a geometric impedance or routing overhead, leading to architectural correspondences between delays and computational costs. Such correspondences belong to Layer 2 and are treated as modeling templates rather than derivations.

8.4 Biological isomorphism: modular geometry and genetic coding

The constitution developed here is substrate-independent at Layer 1: it concerns scan dynamics, finite-resolution projection, and canonical coding. From a Layer 2 perspective, it is therefore natural to ask whether similar constraints could appear in biological information persistence.

Combinatorial capacity. The standard genetic code uses triplets over a four-letter alphabet, yielding $4^3 = 64$ codons, i.e. a 2^6-sized finite readout alphabet. This matches the minimal "small register" intuition: a compact discrete interface can support a large space of effective states under a fixed-length readout rule.

Degeneracy as coarse-graining. The many-to-one mapping from codons to amino acids (plus stop signals) can be viewed as a finite-resolution coarse-graining of the codon alphabet. In the language of O5, such a coarse-graining is naturally modeled by effects that identify multiple micro-labels into a single operational outcome. The wobble mechanism in codon–anticodon pairing provides a concrete biological instance of finite-resolution decoding [42].

Stability as mode selection (hypothesis). One may speculate that the observed structure of the genetic code reflects a selection of robust modes under noise (mutations, translation errors), analogous in spirit to selecting stable eigen-structures under symmetry-preserving dynamics. Quantitative notions of error-minimization and code optimality have been studied in

the biological literature; see, e.g., [43–46]. This analogy is offered as a hypothesis: we do not derive biological optimality from modular/Hecke rigidity in this paper.

Boundary semantics. Under the generative viewpoint of readout, translation can be read as an "execution" of a finite alphabet into a structured outcome space (proteins), rather than a passive storage model. This is a Layer 2 semantic bridge and is not used as a premise in the mathematical constitution.

8.5 Diagonalization perspective: eigen-frames and apparent chaos

The constitution emphasizes that "disorder" can be an artifact of projection. In an abstract Hilbert-space language, a change of basis is a unitary rotation of coordinates: the same object may look complicated in one basis and simple in another. This motivates an interpretation-layer *diagonalization perspective*.

Hecke eigenforms as stable directions. The Hecke algebra is a commuting family on appropriate modular-form spaces (Section 6.1). Hence there exists a basis of simultaneous eigenvectors (eigenforms) in which all Hecke operators act diagonally, and the prime-indexed generators T_p determine the full action. In this sense, "prime anchors" are not eigenvectors themselves but the canonical *generator labels* that select and propagate eigen-data across scales. The resulting picture is that arithmetic rigidity is clearest when one works in the eigenform frame.

Projection creates complexity. Operational readout is, by design, a finite-resolution projection (O5). Projecting an intrinsically unitary scan onto a lower-dimensional discrete interface can produce complex, seemingly irregular patterns even when the underlying evolution is structurally simple. The hologram analogy provides an intuition: a clean image can be encoded in a high-frequency interference pattern and recovered only under an appropriate reconstruction protocol.

Geodesics and "the right angle" (template). On the modular surface, geodesic flow provides a canonical notion of "straightness" in hyperbolic geometry, while coordinate charts and tilings can make trajectories appear intricate. In the same spirit, choosing a cross-section/basis aligned with the relevant commuting structure can be viewed as choosing the "right angle" for diagonalization.

Limits from noncommutativity. The diagonalization viewpoint has intrinsic limits: the scan Weyl pair is noncommutative (O6), and simultaneous eigenvectors for U_{scan} and V do not exist when $\alpha \notin \mathbb{Q}$ (Appendix B.2). Thus, "perfect alignment" cannot eliminate complementarity at Layer 1; it only clarifies which structures can be diagonalized (Hecke) and which cannot (Weyl scan–phase).

8.6 Prism perspective: source, dispersion, spectrum, refocusing

The epigraph of this paper proposes a second semantic picture: *the universe as a prism*. This subsection records the mapping as an interpretation-layer template only.

The source point. In the constitution, the distinguished "point" is the unique cusp class on $X(1)$ (Section 3.3): it is where the canonical local parameter q is defined and where q-expansions are anchored. Any identification of this cusp with a physical singularity or horizon belongs to Layer 2 and is not used as a premise.

Dispersion as an expansion interface. The q-expansion (Section 5.1) maps a continuous analytic object to a discrete coefficient sequence. In the prism vocabulary, this is the dispersion step: what is "undifferentiated" prior to readout becomes a discrete spectrum of coefficient labels once projected through the cusp interface. Finite-resolution readout corresponds to a band-limited or truncated access to that spectrum (O5).

Continuum phase and the apparent information imbalance (template). The prism picture invites a "compression paradox": a single continuous phase parameter (a real angle, or a cusp coordinate τ) ranges over a continuum, while any explicit readout record is necessarily discrete (coefficients, labels, bitstrings). In set-theoretic terms, the continuum has cardinality $2^{\aleph_0}$ while discrete labels live in countable families. The constitution resolves the tension operationally: O2 bounds effective degrees of freedom, and O5 restricts access to finite-resolution effects, so only a finite prefix/bandwidth of the dispersed spectrum is ever accessible. Thus "more information in a point" is a semantic statement about infinite-precision idealization and phase sensitivity, not a claim that a finite observer can extract unbounded information from a physical point.

A prime spectrum. The Hecke/prime skeleton makes the spectral analogy concrete: primes generate the Hecke algebra and appear as the local factors in Euler products (Section 6.4). In this picture, primes act as "primary colors" indexing irreducible building blocks, while eigenforms are the stable directions in which the commuting symmetry acts diagonally.

Computation as refocusing (template). If readout produces scattered coefficient data, then "computation" can be interpreted as the controlled inverse step: using a finite protocol (coding, windowing, and symmetry constraints) to refocus discrete readout back toward a generating object. Mathematically, this borrows the general inverse-problem intuition that global structure can be reconstructed from spectral data, but no specific physical inverse-scattering claim is made here.

9 Quantitative closure: standard theorems and bounds

As a closed constitution, the present framework is only as strong as its *quantitative* consequences. Here we record standard theorems (with explicit constants where possible) and the constant-bearing bounds used throughout the paper.

9.1 From unitary scan to induced measures: equidistribution

Under O5/O6 the scan orbit is an irrational rotation. Weyl's equidistribution theorem implies that the orbit induces the Lebesgue measure on $\mathbb{R}/\mathbb{Z}$ [25, 39]; in particular, for any interval window W,

$$\frac{1}{N}\sum_{t=0}^{N-1}\mathbf{1}_W(x_t)\to|W|. \tag{57}$$

Thus the limiting "probabilities" of window readout are not postulated but induced by the scan dynamics and the chosen finite-resolution window.

Digit statistics from the modular-geodesic coding. Section 4.4 identifies continued-fraction digits as return-symbols of modular geodesics. The Gauss map admits a canonical invariant measure and a closed-form digit law (Theorem 4.3), so digit frequencies are quantitatively constrained for typical orbits. Beyond almost-everywhere digit frequencies, the Gauss–Kuzmin theorem provides a finite-time relaxation guarantee: for broad absolutely continuous

initial laws, the distribution of G^n converges exponentially fast to the Gauss invariant measure (Theorem 4.4). Metrical continued-fraction theory also provides sharp scaling constants (Section 7.2).

Finite-N error control. For any finite set of scan samples $P_N = \{x_0, \dots, x_{N-1}\}$ and any interval window W, the Koksma inequality gives an explicit finite-N bound

$$\left| \frac{1}{N} \sum_{t=0}^{N-1} \mathbf{1}_W(x_t) - |W| \right| \le 2\, D_N^*(P_N), \tag{58}$$

see Appendix B.6. In particular, on convergent lengths the closed-form expressions in Proposition B.2 turn induced probability into a constant-controlled estimate. More generally, the Ostrowski/Zeckendorf coding of the tick count N controls discrepancy via digit sums (Appendix B.7), providing a direct quantitative bridge from canonical coding to finite-N readout accuracy. More precisely, if p_n/q_n are convergents of α and

$$N = \sum_{n=0}^{m} b_n q_n \tag{59}$$

is the Ostrowski expansion of N, then Proposition B.1 gives, for every interval window W,

$$\left| \frac{1}{N} \sum_{t=0}^{N-1} \mathbf{1}_W(x_t) - |W| \right| \le \frac{2}{N} \sum_{n=0}^{m} b_n, \tag{60}$$

hence

$$D_N^*(P_N(\alpha)) \le \frac{2}{N} \sum_{n=0}^{m} b_n. \tag{61}$$

This bound holds for *all* $N \ge 1$ (not only at convergent lengths) and makes the constant explicit. For the golden branch $\alpha = \varphi^{-1}$ at Fibonacci lengths $N = F_n$, Appendix B.10 yields explicit constants: for odd n, $D_{F_n}^* = 1/F_n$ so the window-frequency error is bounded by $2/F_n$; for even n,

$$D_{F_n}^* = \frac{1}{F_n} + \left(1 - \frac{1}{F_n}\right) \frac{1}{\sqrt{5}\, F_n}, \tag{62}$$

so the window-frequency error is bounded by $2\left(1 + \frac{1}{\sqrt{5}}\right) \frac{1}{F_n}$ up to the vanishing factor $(1 - 1/F_n)$. More generally, choosing α with bounded continued-fraction coefficients (constant type) yields an explicit uniform guarantee: if $a_n \le A$ for all n, then Appendix B.7 gives

$$D_N^*(P_N(\alpha)) \le \frac{2A(2 + \log_\varphi N)}{N}, \tag{63}$$

recovering the classical $O((\log N)/N)$ rate with explicit constants. This provides a principled scan-slope selection rule: *bounded partial quotients* give uniformly low discrepancy, and the golden branch ($A = 1$) is the canonical extremal choice compatible with Zeckendorf coding.

9.2 Quantitative discrepancy control and a closed form on convergent lengths

The same irrational-rotation model admits quantitative, non-asymptotic control. The Denjoy–Koksma inequality yields uniform bounds at convergent lengths q_n [18, 47, 48]. More sharply, Proposition B.2 gives a closed form for the one-dimensional star discrepancy at lengths q satisfying $|\alpha - p/q| < 1/q^2$.

For the golden branch $\alpha = \varphi^{-1}$, where the convergents are Fibonacci ratios, this implies an explicit constant:

$$F_n\, D_{F_n}^* \to 1 + \frac{1}{\sqrt{5}} \qquad (n \text{ even}), \tag{64}$$

while $F_n\, D_{F_n}^* = 1$ for odd n.

9.3 Coefficient recovery by scan quadrature: variation bounds and parameter choices

The constitution repeatedly uses the cusp interface as a continuous-to-discrete bridge. To make this quantitative at finite N, it is useful to treat coefficient extraction as a deterministic quadrature problem along a scan orbit, with a discrepancy-controlled error.

Coefficient recovery at height y. Let f be holomorphic on $\mathbb{H}$ and T-periodic, so it admits a q-expansion

$$f(\tau) = \sum_{m \geq 0} a_m q^m, \qquad q = \mathrm{e}^{2\pi \mathrm{i} \tau}. \tag{65}$$

For any $y > 0$, Fourier inversion at height y gives the exact coefficient formula

$$a_n = \mathrm{e}^{2\pi n y} \int_0^1 f(x + \mathrm{i}y)\, \mathrm{e}^{-2\pi \mathrm{i} n x}\, \mathrm{d}x \qquad (n \geq 0). \tag{66}$$

Define the integrand

$$g_{n,y}(x) := f(x + \mathrm{i}y)\, \mathrm{e}^{-2\pi \mathrm{i} n x} \qquad (x \in \mathbb{R}/\mathbb{Z}), \tag{67}$$

so that $a_n = \mathrm{e}^{2\pi n y} \int_{\mathbb{R}/\mathbb{Z}} g_{n,y}\, \mathrm{d}x$.

Scan quadrature estimator and a deterministic finite-N bound. Given a scan orbit $x_t = x_0 + t\alpha \pmod 1$, define the scan-quadrature estimator

$$\widehat{a}_n^{(N)}(y) := \mathrm{e}^{2\pi n y}\, \frac{1}{N} \sum_{t=0}^{N-1} g_{n,y}(x_t). \tag{68}$$

If $g_{n,y}$ has bounded variation, then Koksma's inequality (Appendix B.6) yields

$$\left| \widehat{a}_n^{(N)}(y) - a_n \right| \leq \mathrm{e}^{2\pi n y}\, \mathrm{Var}(g_{n,y})\, D_N^*(P_N(\alpha))\,. \tag{69}$$

Thus, for coefficient recovery the quantitative problem reduces to (i) bounding $\mathrm{Var}(g_{n,y})$ as a function of y and n, and (ii) choosing α, N to control D_N^*.

Proposition 9.1 (Uniform variation bound from the q-expansion)**.** *Let $f(\tau) = \sum_{m \geq 0} a_m q^m$ and $g_{n,y}$ be defined by* (67)*. Then for any $y > 0$,*

$$\mathrm{Var}(g_{n,y}) \leq 2\pi \sum_{m \geq 0} |m - n|\, |a_m|\, \mathrm{e}^{-2\pi m y}. \tag{70}$$

In particular, using $|m - n| \leq m + n$,

$$\mathrm{Var}(g_{n,y}) \leq 2\pi \left(n \sum_{m \geq 0} |a_m|\, \mathrm{e}^{-2\pi m y} \;+\; \sum_{m \geq 0} m\, |a_m|\, \mathrm{e}^{-2\pi m y} \right). \tag{71}$$

Proof. Writing $\tau = x + \mathrm{i}y$ gives

$$g_{n,y}(x) = \sum_{m \geq 0} a_m\, \mathrm{e}^{-2\pi m y}\, \mathrm{e}^{2\pi \mathrm{i}(m-n)x}. \tag{72}$$

Termwise differentiation (justified by absolute convergence for fixed $y > 0$) yields

$$g'_{n,y}(x) = 2\pi \mathrm{i} \sum_{m \geq 0} (m - n)\, a_m\, \mathrm{e}^{-2\pi m y}\, \mathrm{e}^{2\pi \mathrm{i}(m-n)x}. \tag{73}$$

For absolutely continuous 1-periodic functions, $\mathrm{Var}(g_{n,y}) \leq \int_0^1 |g'_{n,y}(x)|\, \mathrm{d}x$, and the triangle inequality gives (70). The bound (71) follows from $|m - n| \leq m + n$. □

An explicit elementary bound for weighted power sums. For integer $s \geq 0$ and $q \in (0,1)$, one has

$$\sum_{m\geq 1} m^s q^m = \frac{q\,P_s(q)}{(1-q)^{s+1}}, \tag{74}$$

where P_s is the Eulerian polynomial of degree s with nonnegative coefficients and $P_s(1) = s!$. Hence

$$\sum_{m\geq 1} m^s q^m \leq \frac{s!\,q}{(1-q)^{s+1}}. \tag{75}$$

See, e.g., [49] for standard generating-function identities and Eulerian-number properties. Below we use (75) with $q = \mathrm{e}^{-2\pi y}$ to turn (70) into explicit y- and n-dependent bounds.

Eisenstein series (level 1). For even $k \geq 4$, the normalized Eisenstein series satisfies

$$E_k(\tau) = 1 - \frac{2k}{B_k} \sum_{m\geq 1} \sigma_{k-1}(m)\, q^m, \tag{76}$$

so $|a_m| \leq C_k\, m^{k-1}$ for $m \geq 1$ with

$$C_k := \left|\frac{2k}{B_k}\right| \zeta(k-1), \tag{77}$$

using $\sigma_{k-1}(m) \leq \zeta(k-1)\, m^{k-1}$. Applying Proposition 9.1 and (75) with $q = \mathrm{e}^{-2\pi y}$ gives the uniform bound

$$\mathrm{Var}(g_{n,y}^{(E_k)}) \leq 2\pi n + 2\pi C_k \left(n\frac{(k-1)!\,q}{(1-q)^k} \;+\; \frac{k!\,q}{(1-q)^{k+1}} \right), \qquad q = \mathrm{e}^{-2\pi y}. \tag{78}$$

Hecke eigen cusp forms (coarse uniform bound). Let $f(\tau) = \sum_{m\geq 1} a_m q^m$ be a normalized Hecke eigen cusp form of even weight k (level 1 for concreteness). Deligne's bound implies $|a_m| \leq d(m)\, m^{(k-1)/2}$. Using the trivial divisor bound $d(m) \leq m+1 \leq 2m$ for $m \geq 1$ yields $|a_m| \leq 2\, m^{(k+1)/2}$, hence Proposition 9.1 and (75) give

$$\mathrm{Var}(g_{n,y}^{(f)}) \leq 4\pi \left(n\frac{s_1!\,q}{(1-q)^{s_1+1}} \;+\; \frac{s_2!\,q}{(1-q)^{s_2+1}} \right), \qquad s_1 := \left\lceil \frac{k+1}{2} \right\rceil, \;\; s_2 := \left\lceil \frac{k+3}{2} \right\rceil, \tag{79}$$

with $q = \mathrm{e}^{-2\pi y}$. For the discriminant form Δ of weight 12, the same bound applies with $s_1 = 7$, $s_2 = 8$.

Choosing α and N (discrepancy control). Given (69), a principled scan-slope choice is to enforce uniformly small D_N^*. The explicit constant-type bound (63) shows that bounded partial quotients ($a_n \leq A$) guarantee $D_N^* = O((\log N)/N)$ with an explicit constant; the golden branch ($A = 1$) yields the canonical smallest bound among constant-type choices and also admits exact discrepancy constants on Fibonacci lengths (Appendix B.10). For generic α with unbounded partial quotients there is no comparable uniform constant, and D_N^* can exhibit spikes at N tied to unusually large continued-fraction digits.

Corollary 9.2 (Constant-type design inequality for coefficient recovery)**.** *Assume the scan slope α has bounded continued-fraction coefficients $a_j \leq A$ for all j (constant type), so that the discrepancy bound* (63) *holds. Then for any T-periodic holomorphic f with q-expansion and for any $y > 0$, the scan-quadrature estimator* (68) *satisfies*

$$\left| \widehat{a}_n^{(N)}(y) - a_n \right| \leq \mathrm{e}^{2\pi n y}\, \mathrm{Var}(g_{n,y})\, \frac{2A(2 + \log_\varphi N)}{N}, \tag{80}$$

where $g_{n,y}$ is defined in (67)*. In particular, for $f = E_k$ one may upper-bound* $\mathrm{Var}(g_{n,y})$ *by* (78)*, and for a normalized Hecke eigen cusp form by* (79)*.*

Joint choice of y and N for a target coefficient index n. The finite-N recovery bound (69) combines (i) an amplification factor $\mathrm{e}^{2\pi ny}$ and (ii) a decay factor in $\mathrm{Var}(g_{n,y})$ driven by $q = \mathrm{e}^{-2\pi y}$. For the polynomial-growth classes above, the small-y asymptotic $q/(1-q)^{s+1} \sim (2\pi y)^{-(s+1)}$ suggests minimizing a proxy of the form $\mathrm{e}^{2\pi ny}\, y^{-p}$, whose optimizer is

Lemma 9.3 (exponential–power tradeoff optimizer)**.** *Let $c > 0$ and $p > 0$. The function $h : (0,\infty) \to (0,\infty)$ given by $h(y) = \mathrm{e}^{cy}\, y^{-p}$ attains its unique minimum at $y = p/c$, and*

$$\min_{y>0} \mathrm{e}^{cy}\, y^{-p} = \mathrm{e}^{p} \left(\frac{c}{p}\right)^{p}. \tag{81}$$

Proof. Differentiate $\log h(y) = cy - p\log y$ to obtain $(\log h)'(y) = c - p/y$, which vanishes if and only if $y = p/c$. Since $(\log h)''(y) = p/y^2 > 0$, this critical point is the unique minimizer. Evaluating at $y = p/c$ gives the stated minimum. □

$$y_\star = \frac{p}{2\pi n}. \tag{82}$$

For Eisenstein series E_k, the dominant term in (78) corresponds to $p = k$; for cusp eigenforms of weight k with the coarse bound (79), the dominant term corresponds to $p \approx s_1 + 1 \approx \frac{k+3}{2}$. Once y is fixed, one selects N so that $D_N^*(P_N(\alpha)) \le \varepsilon/(\mathrm{e}^{2\pi ny}\mathrm{Var}(g_{n,y}))$ for a target tolerance ε, using (63) (or the exact convergent-length formulas) as an explicit design inequality.

Where R1 enters beyond $|q|$ analogy. At the operator level, coefficient recovery and discrepancy control both involve regulated orbit sums of the form $\sum_{t\ge 0} U_{\mathrm{scan}}^t$ applied to mean-zero observables (the cohomological equation for a rotation). The canonical way to make these sums well-defined is precisely Abel/resolvent regularization:

$$\sum_{t\ge 0} r^t\, U_{\mathrm{scan}}^t = (1 - r\, U_{\mathrm{scan}})^{-1}, \qquad 0 < r < 1, \tag{83}$$

followed by the controlled limit $r \uparrow 1$ selecting a finite part (R1; Appendix B.16). In protocol terms, this is the minimal finite-coherence response kernel used to turn formally divergent infinite-time expressions into auditable finite quantities.

Noise terms (explicit). If samples of $g_{n,y}(x_t)$ are corrupted by an additive deterministic error η_t with $|\eta_t| \le \delta$ for all t, then

$$\left|\widehat{a}_n^{(N)}(y) - a_n\right| \le \mathrm{e}^{2\pi ny}\, \mathrm{Var}(g_{n,y})\, D_N^*(P_N(\alpha)) \;+\; \mathrm{e}^{2\pi ny}\, \delta, \tag{84}$$

where the first term is the discrepancy-controlled quadrature error and the second is the amplified measurement perturbation.

Wasserstein bounds versus star discrepancy (why we use discrepancy here). For Lipschitz test functions h on $\mathbb{R}/\mathbb{Z}$, Kantorovich–Rubinstein duality implies $|\frac{1}{N}\sum h(x_t) - \int h| \le \mathrm{Lip}(h)\, W_1(\mu_N, \lambda)$. In one dimension, $W_1(\mu_N,\lambda) = \int_0^1 |F_N(t) - t|\,\mathrm{d}t \le D_N^*(P_N)$, so a Wasserstein-1 bound cannot improve the order of the deterministic discrepancy control unless one has an independent sharp bound on W_1 for the specific orbit. Moreover, for discontinuous window readout $\mathbf{1}_W$ the Lipschitz constant is infinite while $\mathrm{Var}(\mathbf{1}_W) = 2$, so bounded-variation/discrepancy estimates are the natural quantitative language for the scan–projection protocol.

9.4 Hecke rigidity in coefficients: recursion, multiplicativity, and Deligne bounds

For a normalized Hecke eigenform, Hecke commutativity and eigen-structure force strong arithmetic constraints on q-coefficients (Section 6.4). For the discriminant cusp form Δ of weight 12, the coefficients $\tau(n)$ are Hecke eigenvalues and satisfy multiplicativity on coprime indices and prime-power recursions (standard; see [19, 20, 28]). In addition, Deligne's theorem implies the sharp Ramanujan–Petersson bound

$$|\tau(p)| \le 2p^{11/2} \qquad (p \text{ prime}), \tag{85}$$

see Appendix B.11. For completeness, Appendix B.12 derives a standard global growth bound for all integers n from Deligne's prime bound and the prime-power Hecke recursion:

$$|\tau(n)| \le d(n)\, n^{11/2}. \tag{86}$$

Finally, the Euler-product identity for $L(\Delta, s)$ and its absolute convergence for $\Re(s) > 13/2$ are standard consequences of Hecke theory (see, e.g., [19, 20, 28]). Beyond pointwise bounds, mature distribution results constrain normalized prime coefficients. In the non-CM case, Sato–Tate predicts a semicircle law for the normalized values $a_p/(2p^{(k-1)/2})$; see [50–52] for background and broad theorem statements.

Beyond coefficient statistics, there are also deep equidistribution theorems for *Hecke eigenfunctions* on the modular surface (quantum unique ergodicity, and effective variants). Such results are directly relevant whenever one appeals to "stability under Hecke dynamics" or to induced measures associated with Hecke eigenbases; see, e.g., [53] for an effective QUE statement for Hecke–Maaß cusp forms on $\mathrm{SL}_2(\mathbb{Z})\backslash\mathrm{SL}_2(\mathbb{R})$.

How many coefficients determine an eigenform? Sturm bounds and prime reduction. A practical quantitative consequence of Hecke rigidity is that *finitely many* coefficients determine a modular form. Sturm's theorem gives an explicit cutoff: if $f, g \in M_k(\Gamma_0(N))$ satisfy $a_n(f) = a_n(g)$ for all $1 \le n \le B_{k,N}$, where

$$B_{k,N} := \left\lfloor \frac{k}{12} \left[\mathrm{SL}_2(\mathbb{Z}) : \Gamma_0(N)\right] \right\rfloor, \tag{87}$$

then $f = g$ [28,54]. In particular, for level 1 one has $[\mathrm{SL}_2(\mathbb{Z}) : \Gamma_0(1)] = 1$, so matching coefficients up to $\lfloor k/12 \rfloor$ is enough to identify a form.

For normalized Hecke eigenforms, the Hecke relations further reduce the amount of *independent* data needed: knowing the prime eigenvalues a_p for primes $p \le B_{k,N}$ determines a_{p^r} by the prime-power recursion and then determines all a_n with $n \le B_{k,N}$ by multiplicativity. Thus one can, in principle, reconstruct (or validate) an eigenform up to the Sturm bound using only as many prime-indexed constraints as there are primes $p \le B_{k,N}$, providing a concrete quantitative meaning of the "prime skeleton" as a compression mechanism.

9.5 Modular invariance of j and truncation error control

The j-invariant is $\mathrm{PSL}_2(\mathbb{Z})$-invariant by construction; in particular, $j(\tau) = j(-1/\tau)$ [19, 20]. When E_4, E_6 are evaluated via truncated q-series (absolutely convergent for $|q| < 1$), truncation errors admit explicit tail bounds that decay essentially geometrically in the truncation depth N at fixed τ (Appendix B.13). Moreover, Appendix B.14 gives a certified truncation-only error propagation bound for the induced j-invariant error. Since

$$j(\tau) = 1728\, \frac{E_4(\tau)^3}{E_4(\tau)^3 - E_6(\tau)^2} = \frac{E_4(\tau)^3}{\Delta(\tau)}, \tag{88}$$

numerical sensitivity is amplified near the cusp where $|\Delta(\tau)|$ is small, so any finite truncation or finite-precision evaluation should be interpreted through explicit tail bounds and stability estimates.

9.6 A worked end-to-end instance: scan, window readout, cusp evaluation, Hecke checks, and coding

This subsection records one explicit "toy instance" that runs through the full constitution chain with no interpretive steps: a concrete scan model, a concrete finite-resolution instrument, an explicit cusp evaluation of standard modular objects with certified truncation control, prime-skeleton checks on coefficient data, and a canonical tick-time coding.

Step 1: a covariant scan model and an effective observer state. Use the canonical covariant model of O6 on $L^2(\mathbb{R}/\mathbb{Z})$ (Section 2.2): $(U_{\mathrm{scan}}\psi)(x) = \psi(x+\alpha)$, $(V\psi)(x) = \mathrm{e}^{2\pi \mathrm{i} x}\psi(x)$ with $\alpha \notin \mathbb{Q}$. For the commutative subalgebra generated by functions of the phase x, fix an effective observer state given by Lebesgue integration,

$$\omega_{\mathrm{eff}}(g) = \int_{\mathbb{R}/\mathbb{Z}} g(x)\,\mathrm{d}x, \tag{89}$$

which is the invariant state naturally induced by unique ergodicity of irrational rotation.

Step 2: an explicit finite-resolution instrument (POVM by interval windows). Fix an integer $K \geq 1$ (resolution $\varepsilon := 1/K$) and partition $\mathbb{R}/\mathbb{Z}$ into K disjoint intervals

$$I_k^{(\varepsilon)} = [k\varepsilon, (k+1)\varepsilon) \qquad (k = 0, \ldots, K-1), \tag{90}$$

and define effects $E_k^{(\varepsilon)} = \mathbf{1}_{I_k^{(\varepsilon)}}$ (multiplication operators in the x-representation). Then

$$P_k^{(\varepsilon)} = \omega_{\mathrm{eff}}\Big(E_k^{(\varepsilon)}\Big) = \varepsilon, \tag{91}$$

so the protocol-level limiting probabilities are fixed by the geometry of the window family, not postulated. For a finite sample of N scan ticks, the empirical frequencies satisfy the constant-controlled bound

$$\left| \frac{1}{N} \sum_{t=0}^{N-1} \mathbf{1}_{I_k^{(\varepsilon)}}(x_t) - \varepsilon \right| \leq 2\, D_N^*(P_N), \tag{92}$$

by Koksma (Appendix B.6), with explicit closed forms at convergent lengths (Proposition B.2).

Step 3: a canonical tick length and coding choice. Specialize to the golden branch $\alpha = \varphi^{-1}$ and take a Fibonacci length $N = F_n$. Then Appendix B.10 supplies explicit constants for $D_{F_n}^*$, turning the scan–projection statistics into an auditable finite-N estimate. The same choice aligns with Zeckendorf coding (Section 7.3): N admits a unique Fibonacci-digit representation with a locally checkable admissibility rule (no adjacent 1's), and the corresponding digit sums control discrepancy via Appendix B.7.

Step 4: cusp evaluation with certified truncation control. Fix an imaginary part $y > 0$ and define a modular coordinate along the scan by

$$\tau_t := x_t + \mathrm{i}y, \qquad q_t := \mathrm{e}^{2\pi \mathrm{i} \tau_t} = \mathrm{e}^{-2\pi y}\, \mathrm{e}^{2\pi \mathrm{i} x_t}. \tag{93}$$

Evaluate $E_4(\tau_t), E_6(\tau_t)$ by truncated q-series (truncation depth M) and form the induced approximation $j^{(M)}(\tau_t)$. Appendix B.13 and Appendix B.14 provide certified truncation-only error bounds, so modular invariance checks such as

$$j(\tau_t) = j(-1/\tau_t) \tag{94}$$

can be turned into finite-truncation numerical audits with explicit stability budgets (Section 9.5).

Step 5: prime-skeleton checks on coefficient data. For the discriminant form $\Delta(q) = \sum_{n\geq 1} \tau(n)\, q^n$, Hecke eigen-structure implies exact arithmetic constraints: multiplicativity on coprime indices and the prime-power recursion

$$\tau(p^{r+1}) = \tau(p)\,\tau(p^r) - p^{11}\tau(p^{r-1}) \qquad (r \geq 1), \tag{95}$$

see Section 9.4. As concrete consistency checks (all exact integer identities),

$$\tau(6) = \tau(2)\tau(3) = (-24)(252) = -6048, \tag{96}$$

$$\tau(4) = \tau(2)^2 - 2^{11} = 576 - 2048 = -1472, \tag{97}$$

and

$$\tau(9) = \tau(3)^2 - 3^{11} = 63504 - 177147 = -113643. \tag{98}$$

In any model where discrete readout is hypothesized to expose coefficient data of a Hecke eigenform (even after coarse-graining), such relations supply sharp, prime-indexed cross-scale constraints that can be audited at finite depth.

9.7 Discrimination tasks, noise models, and explicit error budgets (conditional falsifiability)

This paper is a constitution rather than a complete laboratory theory, so "falsifiable" must be read in the conditional sense: once one posits a concrete lab-to-protocol mapping (what plays the role of the pointer phase x, what instrument family realizes $\{E_k^{(\varepsilon)}\}$, and how coarse-graining is implemented), the protocol makes checkable quantitative claims that can fail on data.

A minimal set of discrimination tasks. The following tests are designed to discriminate structured scan–projection readout from generic stochastic readout models:

1. **Window statistics with constant-controlled finite-N error.** For chosen windows W (or a window partition), compare empirical frequencies to the induced limiting probabilities, using discrepancy bounds (Section 9.1–9.2). The point is not merely convergence but the availability of explicit constants at special lengths (e.g. Fibonacci lengths on the golden branch).

2. **Sturmian/low-complexity signatures for binary thresholds.** For a binary readout $s_t = \mathbf{1}_W(x_t)$, the irrational-rotation protocol yields a Sturmian mechanical word (Section 7.1) with rigid combinatorial constraints (balance, minimal complexity). Generic i.i.d. noise does not reproduce these constraints except in degenerate limits.

3. **Cross-resolution consistency under canonical coarse-graining.** If an experimental knob changes resolution by an integer factor (e.g. aperture/threshold coarsening), then protocol-level coarse-graining predicts compatibility relations between fine and coarse statistics. On the boundary, a canonical model is the fiber-average operator $\mathcal{C}_n$ of (45); on the modular stage, the corresponding symmetry-preserving cross-scale family is organized by Hecke operators (Section 6.3).

4. **Prime-skeleton constraints when coefficient data is claimed.** In any model that identifies readout with coefficient data of a Hecke eigenform (even approximately), multiplicativity and prime-power recursions supply stringent internal consistency checks (Section 9.4). These constraints are sharply discriminative: they are not generic properties of arbitrary integer sequences.

5. **Protocol fitting and audit-ready parameter extraction.** Once a concrete lab-to-protocol mapping is specified (what is x, what family realizes the windows), one can fit protocol parameters with deterministic finite-N guarantees and test Sturmian/three-gap/Hecke signatures as falsifiers; see Appendix C.

A quantitative noise/decoherence interface. At Layer 1, noise enters by deforming either the effective state ω_{eff} or the effects $\{E_k^{(\varepsilon)}\}$. In the Heisenberg picture, one may represent an instrument/noise channel by a completely positive unital map $\mathcal{N}$ on the observer algebra and write

$$P_k^{(\varepsilon)} = \omega_{\text{eff}}\Big(\mathcal{N}\Big(E_k^{(\varepsilon)}\Big)\Big). \tag{99}$$

Two canonical toy deformations capture common laboratory imperfections:

- **Finite aperture / window smoothing.** Replace a sharp window $\mathbf{1}_W$ by a smoothed kernel $w_{W,\sigma} = \kappa_\sigma * \mathbf{1}_W$ (convolution on $\mathbb{R}/\mathbb{Z}$). This models finite spatial/phase resolution. In discrepancy bounds, the variation $V(\mathbf{1}_W) = 2$ is replaced by $V(w_{W,\sigma}) \le 2$, improving finite-N constants when the aperture is smooth.
- **Finite coherence / exponential memory.** Replace uniform time-averages by Abel-weighted averages $(1-r)\sum_{t\ge 0} r^t(\cdot)$, which is the canonical resolvent regularization of the scan dynamics (R1 and Appendix B.16). This models a causal finite-memory response with exponential forgetting. The limit $r \uparrow 1$ is an idealized infinite-coherence limit.

Error-budget template. In a commutative phase-window model, an auditable total error budget takes the additive form

$$\left|\widehat{P}_W - P_W\right| \;\le\; V(w_{W,\sigma})\, D_N^*(P_N) \;+\; \delta_{\text{instr}}(\sigma) \;+\; \delta_{\text{num}}(M,\tau), \tag{100}$$

where the first term is the deterministic finite-N discrepancy contribution, δ_{instr} collects instrument-model mismatch (e.g. calibration error beyond the smoothing kernel), and δ_{num} is a certified truncation/precision term when modular objects are evaluated via finite q-series depth M (Appendix B.13 and Appendix B.14). The key point is methodological: each contribution can be made explicit and independently audited.

10 Conclusion: geometry as source code (under strict layering)

Under the strict layering discipline of Section 2, the *Ramanujan holographic scanning principle* may be summarized as three constitution clauses:

1. **Time** is the iteration count of an intrinsic unitary scan (O1, O3, O6).
2. **Probability** is an induced measure produced by finite-resolution projection readout (O5), not an external sampling postulate.
3. **Discreteness** is a cusp interface: q-expansions produce arithmetic coefficient data, constrained by Hecke/prime structure and encoded canonically via Ostrowski/Zeckendorf (Sections 5–7).

In this sense, HPA is not an auxiliary coding trick but the minimal arithmetic implementation of modular geometry under finite-resolution readout, and the Ω framework supplies an ontological container compatible with finite information and holographic encoding. The proposed chain is mathematically coherent and computationally checkable.

At Layer 2, one may read the constitution more broadly: readout is a form of *generative calculation* (rendering by scan–projection), and similar finite-resolution coding principles might constrain information persistence across substrates, including biological implementations. Such interpretations are deliberately segregated and do not enter the Layer 0/1 closure.

Remark 10.1 (Final interpretation-layer remark: the modular kaleidoscope)**.** *As an interpretation-layer metaphor (Layer 2), one may summarize the worldview behind HPA–Ω in a single picture. The "ontic" substrate is taken to be continuous unitary modular flow ("light" in a poetic sense), while discreteness arises only at the readout interface: finite-resolution projection breaks continuity into operational labels, and in the modular setting this interface is canonically anchored at cusps via q-expansions (Sections 3 and 5). In the prism vocabulary of the epigraph, the cusp interface disperses "white" unitary flow into a discrete coefficient spectrum, and computation is the protocol-level refocusing step that organizes those labels back toward a generating object (Section 8.6). The modular group then acts as a hyperbolic kaleidoscope: a single fundamental region is replicated and folded across the domain by arithmetic symmetry (Section 3.3). Cross-scale rigidity is organized by the Hecke algebra, whose prime-generated structure propagates to all composite scales (Section 6). In this view, what we call "physics" is, at its core, a disciplined calculus of transformations and induced measures on arithmetic geometry. This remark is interpretive and does not enter the Layer 0/1 closure.*

A Logical closure and dependency chain (audit table)

To make the argument auditable, we list the dependency chain explicitly. Items marked "interpretation layer" are not used as premises.

A.1 Layering axioms (A0; accepted as constitutive)

- O1–O4: ontological container (static global state, finite information, causally local discrete update, holographic map).
- O5–O6 and R1: scan–projection readout, induced measures, Weyl pair, and a fixed finite-part convention.
- Stage choice: adopt the level-1 modular quotient $X(1)$ as a minimal arithmetic-geometric stage under the selection criteria of Section 3.1 (with alternatives left open).

A.2 From axioms to the minimal scan model (A1; standard)

- Weyl pair ⇒ rotation algebra closure (Section 4.1).
- Covariant model ⇒ circle rotation scan $x_t = x_0 + t\alpha \pmod 1$ (O5/O6).

A.3 From scan to discrete coding (A2; standard)

- Irrational rotation + interval window ⇒ Sturmian mechanical word (Section 7.1).
- Continued fraction ⇒ Ostrowski numeration; golden branch ⇒ Zeckendorf degeneration (Section 7.2–7.3).
- Denjoy–Koksma + Ostrowski block decomposition ⇒ finite-N discrepancy bounds controlled by digit sums (Appendix B.7).
- Protocol identification templates for finite readout records (Sturmian/three-gap/Hecke audits) are recorded in Appendix C.

A.4 Arithmetic-geometric mother space (A3; standard definitions and a minimal choice)

- Minimal selection criteria for $X(1)$ and explicit alternatives (Section 3.1).

- $\mathrm{PSL}_2(\mathbb{Z})$ action on $\mathbb{H}$, fundamental domain, cusp identification (Section 3.3).
- Modular-form q-expansion at cusps and Hecke algebra structure (Sections 5.1–6.2).

A.5 Interpretation-layer mappings (A4; not premises)

- "discrete matter = q-coefficients" is a readout-interface hypothesis;
- "S-inversion as wormhole/entanglement template" is a semantic analogy;
- Hecke correspondences as symmetry-preserving coarse-graining are a canonical operator family once the modular stage and cusp interface are adopted (Section 6.3); interpreting Hecke dynamics as physical renormalization requires additional dynamical closure beyond the constitution.

The constitution-level dependency chain may be summarized as

$$\begin{aligned}&\text{scan–projection (O5/O6)} \ \wedge\ \text{cusp interface (q-expansion)} \ \wedge\ \text{Hecke/prime skeleton}\\ &\Rightarrow\ \text{canonical discrete readout with arithmetic rigidity.}\end{aligned} \tag{101}$$

B Mathematical notes (proof sketches)

B.1 Hecke prime-power recursion and prime generation

Starting from the multiplication relation (43), take $m = p^r$ and $n = p$ for a prime p. Using the divisors $d \mid (p^r, p)$, i.e. $d \in \{1, p\}$, one obtains

$$T_{p^r} T_p = T_{p^{r+1}} + p^{k-1} T_{p^{r-1}}, \tag{102}$$

which rearranges to the prime-power recursion (44):

$$T_{p^{r+1}} = T_p T_{p^r} - p^{k-1} T_{p^{r-1}}. \tag{103}$$

This shows all T_{p^r} are generated by T_p, and together with (43) it implies that the full Hecke algebra is generated by $\{T_p\}_{p \text{ prime}}$.

B.2 Weyl pairs and intrinsic incompatibility

Suppose $UV = \mathrm{e}^{2\pi \mathrm{i} \alpha} VU$ with $\alpha \notin \mathbb{Q}$. If ψ were a common eigenvector, $U\psi = \lambda\psi$ and $V\psi = \mu\psi$, then

$$UV\psi = \lambda\mu\psi, \qquad VU\psi = \mu\lambda\psi, \tag{104}$$

but the Weyl relation forces $\lambda\mu = \mathrm{e}^{2\pi \mathrm{i} \alpha}\mu\lambda$, hence $(1 - \mathrm{e}^{2\pi \mathrm{i} \alpha})\lambda\mu = 0$. Since $\alpha \notin \mathbb{Q}$, $\mathrm{e}^{2\pi \mathrm{i} \alpha} \neq 1$, so $\lambda\mu = 0$, impossible for unitary eigenvalues. Thus no nonzero vector can be a simultaneous eigenvector of U and V.

B.3 Why local admissibility constraints matter

Ostrowski/Zeckendorf representations impose local admissibility rules (e.g. Zeckendorf's "no adjacent 1"). These rules turn a global integer representation into a locally checkable grammar. In finite-resolution and quasi-local settings, this locality is essential: a readout protocol that cannot be implemented by local checks is not physically actionable for a finite observer sector.

B.4 Weyl equidistribution and induced frequencies

Let $\alpha \notin \mathbb{Q}$ and consider the irrational rotation on $\mathbb{R}/\mathbb{Z}$,

$$x_t = x_0 + t\alpha \pmod 1. \tag{105}$$

Weyl's equidistribution theorem states that the orbit is uniformly distributed modulo 1 [25,39]. In particular, for any interval $I \subset \mathbb{R}/\mathbb{Z}$,

$$\frac{1}{N}\#\{0 \le t \le N-1 : x_t \in I\} \to |I| \qquad (N \to \infty), \tag{106}$$

where $|I|$ denotes Lebesgue measure. This gives a protocol-level justification of induced frequencies: window readout asymptotically induces the Lebesgue measure.

B.5 Denjoy–Koksma inequality (quantitative control at convergents)

Let $\alpha \notin \mathbb{Q}$ and let p_n/q_n be the convergents of its continued fraction. For a function f of bounded variation on $\mathbb{R}/\mathbb{Z}$, the Denjoy–Koksma inequality states that for all $x \in \mathbb{R}/\mathbb{Z}$,

$$\left| \sum_{t=0}^{q_n-1} f(x + t\alpha) - q_n \int_{\mathbb{R}/\mathbb{Z}} f \, \mathrm{d}x \right| \le \mathrm{Var}(f), \tag{107}$$

see [18,47,48]. For an interval indicator $f = \mathbf{1}_I$, one has $\mathrm{Var}(f) = 2$, hence the deviation of visit counts at length q_n is uniformly bounded by 2.

B.6 Koksma inequality: discrepancy controls readout error

Let $P = \{x_0, \ldots, x_{N-1}\} \subset [0,1)$ be a finite point set and let $f : [0,1] \to \mathbb{R}$ be of bounded variation $\mathrm{Var}(f)$. The one-dimensional Koksma inequality states that

$$\left| \frac{1}{N} \sum_{i=0}^{N-1} f(x_i) - \int_0^1 f(x) \, \mathrm{d}x \right| \le \mathrm{Var}(f)\, D_N^*(P), \tag{108}$$

where $D_N^*(P)$ is the star discrepancy of P [39]. For window readout $f = \mathbf{1}_I$ (an interval indicator), $\mathrm{Var}(f) = 2$, hence

$$\left| \frac{1}{N} \sum_{i=0}^{N-1} \mathbf{1}_I(x_i) - |I| \right| \le 2\, D_N^*(P). \tag{109}$$

This provides a direct quantitative bound that upgrades "induced probability" to a finite-N error-controlled statement.

B.7 Ostrowski block decomposition: discrepancy controlled by coding digits

Let $\alpha \notin \mathbb{Q}$ and let p_n/q_n be the convergents of its continued fraction. Every integer $N \ge 1$ admits an Ostrowski expansion

$$N = \sum_{n=0}^{m} b_n q_n, \tag{110}$$

with digits b_n satisfying standard admissibility constraints (Section 7.2). This expansion yields a natural block decomposition of the first N scan ticks into $\sum_n b_n$ blocks of convergent lengths.

Proposition B.1 (Bounded-variation error bound via Ostrowski digits)**.** *Let f have bounded variation* $\mathrm{Var}(f)$ *on $\mathbb{R}/\mathbb{Z}$. Then for any $x \in \mathbb{R}/\mathbb{Z}$,*

$$\left| \sum_{t=0}^{N-1} f(x + t\alpha) - N \int_{\mathbb{R}/\mathbb{Z}} f \, \mathrm{d}x \right| \le \mathrm{Var}(f) \sum_{n=0}^{m} b_n. \tag{111}$$

Proof. Write $N = \sum_{n=0}^{m} b_n q_n$ and partition the interval of ticks $\{0, 1, \ldots, N-1\}$ into consecutive blocks of lengths q_n, repeated b_n times in any order consistent with the sum. Since the Denjoy–Koksma inequality (Appendix B.5) is uniform in the starting point, each block of length q_n contributes an error of at most $\mathrm{Var}(f)$ relative to its expected value $q_n \int f$. Summing over all blocks gives the stated bound. □

Consequence for star discrepancy. Taking $f = \mathbf{1}_I$ (interval indicator) gives $\mathrm{Var}(f) = 2$, hence for every interval I,

$$\left| \frac{1}{N} \sum_{t=0}^{N-1} \mathbf{1}_I(x + t\alpha) - |I| \right| \leq \frac{2}{N} \sum_{n=0}^{m} b_n, \tag{112}$$

so

$$D_N^*(P_N(\alpha)) \leq \frac{2}{N} \sum_{n=0}^{m} b_n. \tag{113}$$

Thus, at finite N, discrepancy is quantitatively controlled by the *digit sum* of the canonical Ostrowski encoding of tick time.

Golden specialization. For $\alpha = \varphi^{-1}$, the Ostrowski system degenerates to Zeckendorf: $q_n = F_n$ and $b_n \in \{0, 1\}$ with no adjacent 1's. Then $\sum b_n$ is exactly the Zeckendorf Hamming weight $w_Z(N)$, yielding

$$D_N^* \leq \frac{2\, w_Z(N)}{N}. \tag{114}$$

Since the largest Fibonacci index used in the Zeckendorf decomposition satisfies $F_k \leq N < F_{k+1}$ and the no-adjacency constraint gives $w_Z(N) \leq (k+1)/2$, a crude explicit bound is

$$D_N^* \leq \frac{3 + \log_\varphi N}{N}, \tag{115}$$

using $F_k \geq \varphi^{k-2}$ for $k \geq 2$.

Bounded partial quotients (constant type). More generally, if α has bounded continued-fraction coefficients $a_n \leq A$, then Ostrowski digits satisfy $b_n \leq a_{n+1} \leq A$, hence $\sum_{n=0}^{m} b_n \leq A(m+1)$. Since $q_{n+1} = a_{n+1} q_n + q_{n-1} \geq q_n + q_{n-1}$, one has $q_n \geq F_n$ and therefore $m \leq 1 + \log_\varphi N$ whenever $q_m \leq N < q_{m+1}$. Combining these gives an explicit bound

$$D_N^* \leq \frac{2A(2 + \log_\varphi N)}{N}, \tag{116}$$

which recovers the standard $O((\log N)/N)$ discrepancy estimate for constant-type rotations (cf. [39]).

B.8 The three-distance (three-gap) theorem

For $\alpha \notin \mathbb{Q}$ and $N \geq 1$, the sorted set of points $\{t\alpha\}$ $(t = 0, \ldots, N-1)$ partitions the circle into N gaps whose lengths take at most three distinct values (the three-distance theorem). A classical reference is [55].

B.9 Exact star discrepancy at convergent lengths (closed form)

For a point set $P = \{x_0, \ldots, x_{N-1}\} \subset [0, 1)$, the one-dimensional star discrepancy is

$$D_N^*(P) = \sup_{t \in [0,1]} \left| \frac{1}{N} \#\{x_i < t\} - t \right|. \tag{117}$$

Proposition B.2 (Convergent-length star discrepancy for a Kronecker orbit)**.** *Let $\alpha \in (0,1)\setminus\mathbb{Q}$ and let p/q be a reduced rational with*

$$0 < \left|\alpha - \frac{p}{q}\right| < \frac{1}{q^2}. \tag{118}$$

Consider the Kronecker point set

$$P_q(\alpha) := \{\{t\alpha\} : t = 0, 1, \ldots, q-1\} \subset [0,1). \tag{119}$$

Then

$$D_q^*(P_q(\alpha)) = \begin{cases} \dfrac{1}{q}, & \dfrac{p}{q} < \alpha, \\ \dfrac{1}{q} + (q-1)\left(\dfrac{p}{q} - \alpha\right), & \dfrac{p}{q} > \alpha. \end{cases} \tag{120}$$

Proof. Write $\delta := \alpha - \frac{p}{q}$ and note that for $0 \le t \le q-1$ one has $|t\delta| < (q-1)/q^2 < 1/q$. Let $r_t \in \{0, 1, \ldots, q-1\}$ be the residue $r_t \equiv tp \pmod q$; since $\gcd(p,q) = 1$, the map $t \mapsto r_t$ is a permutation.

Case 1: $\delta > 0$ **(i.e.** $p/q < \alpha$**).** For each t,

$$\{t\alpha\} = \left\{\frac{tp}{q} + t\delta\right\} = \frac{r_t}{q} + t\delta \in \left[\frac{r_t}{q}, \frac{r_t+1}{q}\right), \tag{121}$$

where the last inclusion uses $0 \le t\delta < 1/q$ and $r_t = q-1$ is interpreted modulo 1. Hence each interval $[j/q, (j+1)/q)$ contains exactly one point of $P_q(\alpha)$. This implies $D_q^*(P_q(\alpha)) \le 1/q$. On the other hand, since $0 \in P_q(\alpha)$, one has $D_q^*(P_q(\alpha)) \ge 1/q$ (take $t \downarrow 0$), so equality holds.

Case 2: $\delta < 0$ **(i.e.** $p/q > \alpha$**).** Let $\delta' := -\delta = \frac{p}{q} - \alpha > 0$. For $t \ge 1$, $r_t \ne 0$ so $r_t/q \ge 1/q$, and

$$\{t\alpha\} = \left\{\frac{tp}{q} - t\delta'\right\} = \frac{r_t}{q} - t\delta' \in \left(\frac{r_t-1}{q}, \frac{r_t}{q}\right), \tag{122}$$

since $0 < t\delta' < 1/q$. Thus every interval $[j/q, (j+1)/q)$ with $j = 0, \ldots, q-2$ contains exactly one point coming from the unique $t \in \{1, \ldots, q-1\}$ with $r_t = j+1$, while the point $0 \in P_q(\alpha)$ lies in $[0, 1/q)$.

Ordering points by increasing bin index j, we can write the sorted list as

$$x_0 = 0, \qquad x_{j+1} = \frac{j+1}{q} - t(j)\delta', \qquad j = 0, 1, \ldots, q-2, \tag{123}$$

where $t(j) \in \{1, \ldots, q-1\}$ is the unique integer satisfying $t(j)p \equiv j+1 \pmod q$. Then

$$\frac{j+2}{q} - x_{j+1} = \frac{1}{q} + t(j)\delta'. \tag{124}$$

Taking the maximum over j and using $\max_j t(j) = q-1$, we obtain

$$D_q^*(P_q(\alpha)) = \max_j \left(\frac{j+2}{q} - x_{j+1}\right) = \frac{1}{q} + (q-1)\delta' \tag{125}$$

as claimed. □

B.10 Golden branch specialization and the $1 + 1/\sqrt{5}$ constant

Let $\varphi = (1 + \sqrt{5})/2$ and $\alpha = \varphi^{-1}$. The convergents of α are ratios of Fibonacci numbers:

$$\frac{p_n}{q_n} = \frac{F_{n-1}}{F_n}. \tag{126}$$

Using Binet's formula $F_n = (\varphi^n - \psi^n)/\sqrt{5}$ with $\psi = (1 - \sqrt{5})/2 = -\varphi^{-1}$, one obtains the exact approximation error

$$\alpha - \frac{F_{n-1}}{F_n} = \frac{(-1)^n}{\sqrt{5}\, F_n^2}. \tag{127}$$

Combining this with Proposition B.2 yields an exact closed form for $D^*_{F_n}$ and, in particular, for even n,

$$F_n\, D^*_{F_n} = 1 + \left(1 - \frac{1}{F_n}\right) \frac{1}{\sqrt{5}} \;\longrightarrow\; 1 + \frac{1}{\sqrt{5}}. \tag{128}$$

B.11 Deligne's bound for Ramanujan $\tau(p)$

For a normalized holomorphic Hecke eigenform of weight k, Deligne proved the Ramanujan–Petersson bound

$$|a_p| \le 2p^{(k-1)/2} \qquad (p \text{ prime}), \tag{129}$$

as a consequence of the Weil conjectures [56]. For the discriminant form Δ of weight 12, this specializes to

$$|\tau(p)| \le 2p^{11/2}. \tag{130}$$

B.12 Prime powers and all integers: a global growth bound for $\tau(n)$

For Δ (weight 12), the Hecke recursion at prime powers reads

$$\tau(p^{r+1}) = \tau(p)\tau(p^r) - p^{11}\tau(p^{r-1}). \tag{131}$$

Define the normalized sequence

$$b_r := \frac{\tau(p^r)}{p^{11r/2}}, \qquad r \ge 0. \tag{132}$$

Then $b_0 = 1$, $b_1 = \tau(p)/p^{11/2}$, and the recursion becomes

$$b_{r+1} = b_1 b_r - b_{r-1}. \tag{133}$$

Under Deligne's bound $|b_1| \le 2$ (Appendix B.11), we can make the growth control completely explicit via Chebyshev polynomials of the second kind. Let U_r be defined by

$$U_0(t) = 1, \qquad U_1(t) = 2t, \qquad U_{r+1}(t) = 2t\, U_r(t) - U_{r-1}(t). \tag{134}$$

Setting $t = b_1/2$ gives the same recurrence and initial data as $\{b_r\}$, hence

$$b_r = U_r\!\left(\frac{b_1}{2}\right). \tag{135}$$

If $|b_1| \le 2$, write $b_1 = 2\cos\theta$ for some $\theta \in [0, \pi]$. Then the standard identity

$$U_r(\cos\theta) = \frac{\sin((r+1)\theta)}{\sin\theta} \tag{136}$$

implies $|U_r(\cos\theta)| \le r + 1$ (use $|\sin((r+1)\theta)| \le (r+1)|\sin\theta|$ and continuity at $\theta = 0, \pi$). Therefore

$$|b_r| \le r + 1, \tag{137}$$

and hence

$$|\tau(p^r)| \le (r+1)\, p^{11r/2}. \tag{138}$$

Using multiplicativity of $\tau(n)$ on coprime indices and writing $n = \prod_i p_i^{r_i}$, we obtain the global bound

$$|\tau(n)| \le \prod_i (r_i+1)\, p_i^{11r_i/2} = d(n)\, n^{11/2}, \tag{139}$$

where $d(n) = \prod_i (r_i+1)$ is the divisor function. In particular, this yields the standard growth form $|\tau(n)| = O(n^{11/2+\varepsilon})$ for any $\varepsilon > 0$.

B.13 Tail bounds for Eisenstein q-series (for numerical error control)

Let $q = \mathrm{e}^{2\pi \mathrm{i}\tau}$ with $|q| = r < 1$. The Eisenstein series have absolutely convergent q-expansions

$$E_4(\tau) = 1 + 240 \sum_{n\ge 1} \sigma_3(n) q^n, \qquad E_6(\tau) = 1 - 504 \sum_{n\ge 1} \sigma_5(n) q^n. \tag{140}$$

Using the bound $\sigma_k(n) \le \zeta(k)\, n^k$ for $k > 1$ (indeed $\sigma_k(n) = \sum_{d|n} d^k \le n^k \sum_{m\ge 1} m^{-k} = \zeta(k)\, n^k$), one obtains explicit truncation bounds. For example, for the N-term truncation $E_4^{(N)}(\tau) := 1 + 240 \sum_{n=1}^{N} \sigma_3(n) q^n$,

$$|E_4(\tau) - E_4^{(N)}(\tau)| \le 240\, \zeta(3) \sum_{n>N} n^3 r^n. \tag{141}$$

The tail sum can be written as

$$\sum_{n>N} n^3 r^n = r^{N+1} \sum_{m\ge 0} (m+N+1)^3 r^m, \tag{142}$$

and expanded using the standard identities for $\sum_{m\ge 0} m^\ell r^m$ ($\ell = 0, 1, 2, 3$). Analogous bounds hold for E_6 with $\zeta(5) \sum_{n>N} n^5 r^n$.

These tail bounds justify the qualitative statement used in Section 9.5: truncated q-series evaluations of E_4, E_6 exhibit essentially geometric decay in N at fixed τ, with constants depending on r and polynomial factors in N.

B.14 Certified truncation bounds for the j-invariant

Fix $\tau \in \mathbb{H}$ and write $q = \mathrm{e}^{2\pi \mathrm{i}\tau}$, $r = |q| < 1$. Let $E_4^{(N)}(\tau), E_6^{(N)}(\tau)$ denote truncations at depth N and let the corresponding tail bounds be

$$|E_4(\tau) - E_4^{(N)}(\tau)| \le \varepsilon_4(\tau; N), \qquad |E_6(\tau) - E_6^{(N)}(\tau)| \le \varepsilon_6(\tau; N), \tag{143}$$

where $\varepsilon_4, \varepsilon_6$ are obtained from the inequalities in Appendix B.13.

Define

$$D(\tau) := E_4(\tau)^3 - E_6(\tau)^2, \qquad D^{(N)}(\tau) := E_4^{(N)}(\tau)^3 - E_6^{(N)}(\tau)^2. \tag{144}$$

Let $M_4 := |E_4^{(N)}(\tau)| + \varepsilon_4(\tau; N)$ and $M_6 := |E_6^{(N)}(\tau)| + \varepsilon_6(\tau; N)$. Then

$$|D(\tau) - D^{(N)}(\tau)| \le 3M_4^2\, \varepsilon_4(\tau; N) + 2M_6\, \varepsilon_6(\tau; N) \;=:\; \delta_D(\tau; N). \tag{145}$$

Consequently, if $|D^{(N)}(\tau)| > \delta_D(\tau; N)$, then $D(\tau) \neq 0$ and

$$|D(\tau)| \ge |D^{(N)}(\tau)| - \delta_D(\tau; N) =: D_{\min}(\tau; N) > 0. \tag{146}$$

Since $j(\tau) = 1728\, E_4(\tau)^3 / D(\tau)$, one obtains the certified truncation bound

$$|j(\tau) - j^{(N)}(\tau)| \le 1728 \left(\frac{3M_4^2\, \varepsilon_4(\tau; N)}{D_{\min}(\tau; N)} \;+\; |E_4^{(N)}(\tau)|^3 \frac{\delta_D(\tau; N)}{D_{\min}(\tau; N)\, |D^{(N)}(\tau)|} \right), \tag{147}$$

where $j^{(N)}$ is computed from the truncated Eisenstein series.

Remark on floating-point saturation. The bound above controls truncation error. In finite-precision arithmetic, observed differences can plateau at a numerical floor once truncation becomes negligible.

B.15 Petersson inner product and self-adjointness of Hecke operators

Let $S_k(\mathrm{PSL}_2(\mathbb{Z}))$ be the space of weight-k cusp forms for $\mathrm{PSL}_2(\mathbb{Z})$. The Petersson inner product is

$$\langle f, g\rangle := \int_{\mathrm{PSL}_2(\mathbb{Z})\backslash\mathbb{H}} f(\tau)\,\overline{g(\tau)}\,(\Im\tau)^k\,\frac{\mathrm{d}x\,\mathrm{d}y}{y^2}, \qquad \tau = x + \mathrm{i}y, \tag{148}$$

which converges for cusp forms. For level 1, the Hecke operator T_n admits the classical explicit formula

$$(T_n f)(\tau) = n^{k-1} \sum_{\substack{ad=n\\ d>0}} \sum_{b \pmod d} d^{-k}\, f\!\left(\frac{a\tau + b}{d}\right), \tag{149}$$

see standard references such as [20, 28].

Self-adjointness (standard). With respect to the Petersson product, the Hecke operators are self-adjoint on cusp forms:

$$\langle T_n f, g\rangle = \langle f, T_n g\rangle, \tag{150}$$

and the family $\{T_n\}$ commutes. A standard proof is by inserting the explicit formula for T_n into the integral and applying a change of variables using the $\mathrm{PSL}_2(\mathbb{Z})$-invariance of the hyperbolic measure $\mathrm{d}x\,\mathrm{d}y/y^2$ together with the automorphy factors (see [28]).

Diagonalization consequence. As commuting self-adjoint operators on the finite-dimensional space $S_k(\mathrm{PSL}_2(\mathbb{Z}))$, the Hecke operators admit an orthogonal basis of simultaneous eigenforms. This justifies the "diagonalization frame" language used in Section 6.4 and in the interpretation-layer discussion (Section 8.5).

B.16 Abel regularization for rotation-orbit sums (R1)

R1 fixes a canonical regulated-to-continuum convention: *Abel first, then limit.* In the rotation setting of O5, this can be stated in a clean, auditable form.

Abel means. Let $\alpha \notin \mathbb{Q}$ and let $f : \mathbb{R}/\mathbb{Z} \to \mathbb{C}$ be continuous. For $0 < r < 1$, define the Abel-weighted orbit average

$$A_r(f; x) := (1 - r) \sum_{t \geq 0} r^t\, f(x + t\alpha), \qquad x \in \mathbb{R}/\mathbb{Z}. \tag{151}$$

Resolvent form (operator-theoretic viewpoint). Let U_α denote the Koopman operator of the rotation $x \mapsto x + \alpha$ on $C(\mathbb{R}/\mathbb{Z})$, i.e. $(U_\alpha g)(x) = g(x + \alpha)$. For $0 < r < 1$ the geometric series converges in operator norm and yields the resolvent identity

$$(1 - r) \sum_{t \geq 0} r^t\, U_\alpha^t = (1 - r)\,(1 - r\,U_\alpha)^{-1}. \tag{152}$$

Thus Abel means are the canonical resolvent regularization of orbit sums for a unitary/measure-preserving evolution: the factor $(1-r)$ extracts the invariant component in the limit $r \uparrow 1$, while oscillatory components are suppressed (as seen explicitly on Fourier modes below).

From a protocol standpoint, the weights r^t may be interpreted as a minimal causal finite-memory response kernel (exponential forgetting). Sending $r \uparrow 1$ corresponds to an idealized infinite-coherence/infinite-memory limit. Then

$$\lim_{r\uparrow 1} A_r(f;x) = \int_{\mathbb{R}/\mathbb{Z}} f(u)\,\mathrm{d}u \tag{153}$$

uniformly in x. A standard proof is by Fourier modes: for $f_m(x) = \mathrm{e}^{2\pi\mathrm{i}mx}$ one has

$$A_r(f_m;x) = (1-r)\mathrm{e}^{2\pi\mathrm{i}mx}\sum_{t\geq 0}\left(r\,\mathrm{e}^{2\pi\mathrm{i}m\alpha}\right)^t = (1-r)\mathrm{e}^{2\pi\mathrm{i}mx}\frac{1}{1-r\,\mathrm{e}^{2\pi\mathrm{i}m\alpha}}, \tag{154}$$

which tends to 0 for $m \neq 0$ and equals 1 for $m = 0$. Trigonometric polynomials follow by linearity and density in $C(\mathbb{R}/\mathbb{Z})$. This is a classical Abel summability mechanism; see [16].

Finite parts for orbit traces. If $\mu := \int f$ is the mean, the unnormalized Abel sum has the canonical decomposition

$$\sum_{t\geq 0} r^t f(x+t\alpha) \;=\; \frac{\mu}{1-r} \;+\; \sum_{t\geq 0} r^t\big(f(x+t\alpha)-\mu\big), \tag{155}$$

where the first term carries the universal divergence as $r \uparrow 1$. R1 selects the *finite part* (when it exists) as

$$\mathrm{FP}(f;x) := \lim_{r\uparrow 1}\sum_{t\geq 0} r^t\big(f(x+t\alpha)-\mu\big). \tag{156}$$

For a trigonometric polynomial $f(x) = \sum_m \widehat{f}_m \mathrm{e}^{2\pi\mathrm{i}mx}$, one obtains the explicit finite part

$$\mathrm{FP}(f;x) = \sum_{m\neq 0} \widehat{f}_m\,\frac{\mathrm{e}^{2\pi\mathrm{i}mx}}{1-\mathrm{e}^{2\pi\mathrm{i}m\alpha}}, \tag{157}$$

which shows how Abel regularization canonically resolves the constant-mode divergence while preserving the nontrivial phase dependence.

B.17 Formal power-series integrality: why $j(q)$ has integer coefficients

Lemma B.3 (unit-constant denominator implies integrality)**.** *Let $A(q), B(q) \in \mathbb{Z}[[q]]$ be formal power series with $B(0) = 1$. Then there exists a unique $C(q) \in \mathbb{Z}[[q]]$ such that*

$$A(q) = B(q)\,C(q), \tag{158}$$

equivalently $C(q) = A(q)/B(q)$ in the ring $\mathbb{Z}[[q]]$.

Proof. Write $A(q) = \sum_{n\geq 0} a_n q^n$, $B(q) = \sum_{n\geq 0} b_n q^n$ with $b_0 = 1$, and seek $C(q) = \sum_{n\geq 0} c_n q^n$. The identity $A = BC$ is equivalent to the coefficient recursion

$$a_n = \sum_{k=0}^{n} b_k c_{n-k}. \tag{159}$$

For $n = 0$ this gives $c_0 = a_0$. For $n \geq 1$, solve uniquely as

$$c_n = a_n - \sum_{k=1}^{n} b_k c_{n-k}, \tag{160}$$

which is an integer since all $a_n, b_k, c_{n-k} \in \mathbb{Z}$. Uniqueness follows from the recursion. □

Application to modular objects. For level 1, the Eisenstein series E_4, E_6 have q-expansions with integer coefficients and constant term 1, and $\Delta = (E_4^3 - E_6^2)/1728$ satisfies $\Delta(q) = q + O(q^2)$ with integer coefficients [19, 20]. Write $\Delta(q) = q\,\Delta_1(q)$ with $\Delta_1(0) = 1$ and $\Delta_1 \in \mathbb{Z}[[q]]$. Then

$$j(q) = 1728\,\frac{E_4(q)^3}{E_4(q)^3 - E_6(q)^2} = \frac{E_4(q)^3}{\Delta(q)} = q^{-1}\,\frac{E_4(q)^3}{\Delta_1(q)}, \tag{161}$$

and Lemma B.3 implies $E_4^3/\Delta_1 \in \mathbb{Z}[[q]]$, hence $j(q) \in q^{-1}\mathbb{Z}[[q]]$.

C Protocol identification and fitting templates (audit-ready)

The constitution is designed to be auditable: once a laboratory-to-protocol mapping is fixed, one should be able to *fit* the protocol parameters and to *falsify* the model by finite-data consistency checks with explicit error budgets. This appendix records deterministic fitting templates that require no stochastic modeling and no simulation assumptions.

C.1 Binary readout from rotation: Sturmian signatures and a slope estimator

Consider the Layer 1 rotation scan of O5,

$$x_t = x_0 + t\alpha \pmod 1, \qquad \alpha \notin \mathbb{Q},$$

and a binary window readout

$$s_t = \mathbf{1}_W(x_t) \in \{0, 1\},$$

for an interval window $W \subset \mathbb{R}/\mathbb{Z}$. It is classical that such codings of irrational rotations by intervals yield Sturmian (mechanical) words [35, 36].

Finite-data Sturmian diagnostics. Given a finite binary record $s_0, \ldots, s_{N-1}$, two standard diagnostics can be used as deterministic consistency checks:

- **Factor complexity.** Let $p(n)$ be the number of distinct length-n subwords among the factors of the observed record. For a Sturmian word, $p(n) = n + 1$ for all $n \geq 1$ [35, 36].
- **Balance.** A Sturmian word is balanced: for any two factors u, v of the same length, the number of 1's differs by at most 1 [36]. Balance yields sharp finite-N constraints on fluctuations of prefix frequencies.

Failure of these diagnostics at small scales is a direct falsifier of the pure rotation+interval-window model, independent of any asymptotic limit.

A canonical slope estimator (when the coding is fixed). To turn binary readout into a concrete "fit", one must fix a coding convention that associates a unique slope to a word. A standard convention is the *(lower) mechanical word* with parameters (α, ρ),

$$w_t(\alpha, \rho) := \lfloor (t+1)\alpha + \rho \rfloor - \lfloor t\alpha + \rho \rfloor \in \{0, 1\}, \tag{162}$$

which is Sturmian for $\alpha \notin \mathbb{Q}$ [36]. In this convention, the limiting frequency of 1's equals α and admits an explicit finite-N deviation bound:

Lemma C.1 (prefix frequency estimates the slope in the mechanical convention)**.** *Let $w_t(\alpha, \rho)$ be defined by* (162) *with $\alpha \in (0, 1)$ and $\rho \in \mathbb{R}$. Let $S_N := \sum_{t=0}^{N-1} w_t(\alpha, \rho)$. Then for every $N \geq 1$,*

$$\left| \frac{S_N}{N} - \alpha \right| \leq \frac{1}{N}. \tag{163}$$

Proof. Summing (162) telescopes: $S_N = \lfloor N\alpha + \rho \rfloor - \lfloor \rho \rfloor$. Hence $|S_N - (N\alpha + \rho - \rho)| \leq 1$, which gives (163). □

Thus, under a fixed mechanical-coding convention, one can fit α from a finite record by $\widehat{\alpha} = S_N/N$ with a deterministic $1/N$ error guarantee.

General interval windows: fitting window length with discrepancy control. If the coding uses an arbitrary interval W of length $|W|$, then the induced limiting frequency is $|W|$ and finite-N deviation is controlled by discrepancy:

$$\left| \frac{1}{N} \sum_{t=0}^{N-1} \mathbf{1}_W(x_t) - |W| \right| \leq 2\, D_N^*(P_N(\alpha))\,, \tag{164}$$

by Koksma (Appendix B.6). If α is of constant type ($a_j \leq A$), then (63) yields an explicit parameter-free bound on D_N^* and therefore on the fit error of $|W|$.

C.2 Phase-level signatures: the three-gap theorem

When the protocol exposes phase samples $\{x_t\}$ (or when multiple thresholds allow partial reconstruction of ordered phase points), the point set $P_N(\alpha) = \{\{t\alpha\} : 0 \leq t \leq N-1\}$ admits a sharp deterministic signature: its complementary gaps take at most three lengths (the three-gap theorem) [55]. This provides an additional finite-data falsifier for the pure Kronecker scan model, independent of any probabilistic assumptions.

C.3 Coefficient-level audits: Hecke recursions as prime-indexed constraints

If a readout sector is hypothesized to expose (exactly or approximately) a coefficient sequence $\{a_n\}$ of a Hecke eigenform, then the prime-skeleton relations supply stringent finite-depth internal consistency tests:

- **Coprime multiplicativity.** $a_{mn} = a_m a_n$ for $(m, n) = 1$.
- **Prime-power recursion.** $a_{p^{r+1}} = a_p a_{p^r} - p^{k-1} a_{p^{r-1}}$ for $r \geq 1$ (weight k).
- **Finite determination (Sturm bound).** Matching coefficients up to the Sturm cutoff determines the modular form [28, 54] (Section 9.4).

These constraints are purely arithmetic identities; they can therefore be used as audit-grade "fit/fail" conditions whenever coefficient claims are made.

D Limitations and open problems

1. **Stage non-uniqueness.** The selection of $X(1)$ is motivated by a minimality principle (Section 3.1), not derived as a unique necessity from O1–O6. Alternative arithmetic stages (higher level modular curves, other arithmetic surfaces, higher-rank automorphic quotients) and even non-arithmetic chaotic stages are not ruled out *a priori*; identifying additional physical constraints that would select (or exclude) such alternatives remains open.
2. **From protocol-level Hecke to micro-dynamics.** Section 6.3 motivates Hecke operators as canonical symmetry-preserving coarse-graining operators once modular symmetry and the cusp interface are adopted. Turning this into a physical law still requires dynamical closure: one must embed the coarse-graining/Hecke structure into a concrete micro-model (e.g. a QCA update rule or an effective Hamiltonian) and derive observable consequences with an explicit error budget.

3. **Regularization is motivated but not forced.** R1 is given a canonical summability/resolvent motivation (Section 2.2 and Appendix B.16), and can be read as a finite-coherence (exponentially forgetting) instrument limit. Nevertheless, the regularization choice is not uniquely compelled; establishing robustness of protocol-level conclusions under alternative admissible kernels (and linking the choice to concrete locality/causality constraints) remains an open methodological problem.

4. **Laboratory mapping of the scan–projection chain.** The scan Weyl pair and the window-POVM model provide a clean Layer 1 abstraction, but an end-to-end quantitative model of a laboratory measurement chain (finite aperture, decoherence, noise, calibration drift, finite sampling) is not developed here. Section 9.7 provides an audit-style template, but concrete platform-specific instantiations are needed for experimental confrontation.

5. **Observer sector and holographic map instances.** The axioms use ω_{eff} (observer-sector effective state) and the holographic map Φ at a general level (O4–O5). While Section 9.6 gives a fully explicit toy instance for the scan/window/cusp/Hecke/coding chain, a detailed micro-dynamical realization of an observer-accessible subalgebra together with an explicit AQEC-style reconstruction map remains to be exhibited and analyzed end-to-end.

6. **Coefficient data as physical readout remains an interface hypothesis.** Treating "discrete matter = q-coefficients" is not a theorem but an interface hypothesis (Section 5). To become predictive, one must specify which families of modular objects (weight, level, character; possibly vector-valued objects) correspond to which physical sectors and provide systematic matching criteria and uncertainty budgets.

7. **Hecke-driven stability and QUE constraints.** When claims involve induced measures or stability properties tied to Hecke eigenstructures on the modular surface, the relevant body of QUE/effective QUE results provides strong constraints (Section 9.4). Integrating those constraints into a concrete readout model, and clarifying which measures are being compared in a given physicalization, remains open.

References

[1] Haobo Ma. Omega theory: Axiomatic foundations of holographic spacetime and interactive evolution. Companion physics manuscript, 2025.

[2] Haobo Ma. Holographic polar arithmetic: Multiplicative ontology, unitary scanning, and the geometric origin of quantum uncertainty. Companion mathematical manuscript, 2025.

[3] Haobo Ma. The motive at infinity: Functorialization of the holographic scanning principle, period realizations, and a selection principle. Companion manuscript, 2025.

[4] Raphael Bousso. The holographic principle. *Reviews of Modern Physics*, 74:825–874, 2002.

[5] P. Arrighi. An overview of quantum cellular automata. *Natural Computing*, 18(4):885–899, 2019.

[6] D. Gross, V. Nesme, H. Vogts, and R. F. Werner. Index theory of one dimensional quantum walks and cellular automata. *Communications in Mathematical Physics*, 310(2):419–454, 2012.

[7] Ahmed Almheiri, Xi Dong, and Daniel Harlow. Bulk locality and quantum error correction in AdS/CFT. *Journal of High Energy Physics*, 2015(4):163, 2015.

[8] Fernando Pastawski, Beni Yoshida, Daniel Harlow, and John Preskill. Holographic quantum error-correcting codes: Toy models for the bulk/boundary correspondence. *Journal of High Energy Physics*, 2015(6):1–55, 2015.

[9] Daniel Harlow. The ryu–takayanagi formula from quantum error correction. *Communications in Mathematical Physics*, 354(3):865–912, 2017.

[10] Karl Kraus. *States, Effects, and Operations: Fundamental Notions of Quantum Theory*, volume 190 of *Lecture Notes in Physics*. Springer, Berlin, 1983.

[11] Michael A. Nielsen and Isaac L. Chuang. *Quantum Computation and Quantum Information*. Cambridge University Press, Cambridge, 2000.

[12] Andrew M. Gleason. Measures on the closed subspaces of a hilbert space. *Journal of Mathematics and Mechanics*, 6(6):885–893, 1957.

[13] Paul Busch. Quantum states and generalized observables: A simple proof of gleason's theorem. *Physical Review Letters*, 91(12):120403, 2003.

[14] Ola Bratteli and Derek W. Robinson. *Operator Algebras and Quantum Statistical Mechanics*. Springer, Berlin, 1997.

[15] Rudolf Haag. *Local Quantum Physics*. Springer, Berlin, 1996.

[16] G. H. Hardy. *Divergent Series*. Clarendon Press, Oxford, 1949.

[17] John G. Ratcliffe. *Foundations of Hyperbolic Manifolds*. Springer, New York, 1994.

[18] Anatole Katok and Boris Hasselblatt. *Introduction to the Modern Theory of Dynamical Systems*. Cambridge University Press, 1995.

[19] Jean-Pierre Serre. *A Course in Arithmetic*. Springer, New York, 1973.

[20] Tom M. Apostol. *Modular Functions and Dirichlet Series in Number Theory*. Springer, New York, 2 edition, 1990.

[21] Marc A. Rieffel. c^*-algebras associated with irrational rotations. *Pacific Journal of Mathematics*, 93(2):415–429, 1981.

[22] Alain Connes. *Noncommutative Geometry*. Academic Press, 1994.

[23] Giuseppe De Nittis and Giovanni Landi. Generalized TKNN-equations. 2011.

[24] Gaetano Fiore and Davide Franco. Modules over the noncommutative torus and elliptic curves. *Letters in Mathematical Physics*, 104:1425–1443, 2014.

[25] Hermann Weyl. Über die gleichverteilung von zahlen mod. eins. *Mathematische Annalen*, 77:313–352, 1916.

[26] Caroline Series. The modular surface and continued fractions. *Journal of the London Mathematical Society*, 31:69–80, 1985.

[27] Marius Iosifescu and Cor Kraaikamp. *Metrical Theory of Continued Fractions*. Springer, Dordrecht, 2002.

[28] Fred Diamond and Jerry Shurman. *A First Course in Modular Forms*. Springer, New York, 2005.

[29] Maxim Kontsevich and Don Zagier. Periods. In Björn Engquist and Wilfried Schmid, editors, *Mathematics Unlimited – 2001 and Beyond*, pages 771–808. Springer, Berlin, 2001.

[30] Goro Shimura. *Introduction to the Arithmetic Theory of Automorphic Functions*. Princeton University Press, Princeton, 1971.

[31] William A. Stein. *Modular Forms: A Computational Approach*, volume 79 of *Graduate Studies in Mathematics*. American Mathematical Society, Providence, RI, 2007.

[32] Pierre Deligne. Valeurs de fonctions l et périodes d'intégrales. In *Automorphic Forms, Representations and L-Functions*, volume 33 of *Proceedings of Symposia in Pure Mathematics*, pages 313–346. American Mathematical Society, Providence, RI, 1979.

[33] Jeffrey A. Harvey, Yichen Hu, and Yuxiao Wu. Galois symmetry induced by hecke relations in rational conformal field theory and associated modular tensor categories. 2019.

[34] Vincent Bouchard, Thomas Creutzig, and Aniket Joshi. Hecke operators on vector-valued modular forms. *SIGMA*, 15:041, 2019.

[35] Marston Morse and Gustav A. Hedlund. Symbolic dynamics II. Sturmian trajectories. *American Journal of Mathematics*, 62(1):1–42, 1940.

[36] M. Lothaire. *Algebraic Combinatorics on Words*. Cambridge University Press, Cambridge, 2002.

[37] Jean-Paul Allouche and Jeffrey Shallit. *Automatic Sequences: Theory, Applications, Generalizations*. Cambridge University Press, Cambridge, 2003.

[38] E. Zeckendorf. Représentation des nombres naturels par une somme de nombres de Fibonacci ou de nombres de Lucas. *Bulletin de la Société Royale des Sciences de Liège*, 41:179–182, 1972.

[39] L. Kuipers and Harald Niederreiter. *Uniform Distribution of Sequences*. Wiley, New York, 1974.

[40] Michael Baake and Uwe Grimm. *Aperiodic Order*. Cambridge University Press, Cambridge, 2013.

[41] Pablo Arrighi, Stefano Facchini, and Marcelo Forets. Discrete lorentz covariance for quantum walks and quantum cellular automata. *New Journal of Physics*, 16(9):093007, 2014.

[42] Francis H. C. Crick. Codon–anticodon pairing: The wobble hypothesis. *Journal of Molecular Biology*, 19(2):548–555, 1966.

[43] David Haig and Laurence D. Hurst. A quantitative measure of error minimization in the genetic code. *Journal of Molecular Evolution*, 33:412–417, 1991.

[44] Stephen J. Freeland and Laurence D. Hurst. The genetic code is one in a million. *Journal of Molecular Evolution*, 47(3):238–248, 1998.

[45] S. J. Freeland and L. D. Hurst. Load minimization of the genetic code: history does not explain the pattern. *Proceedings of the Royal Society of London. Series B: Biological Sciences*, 265(1410):2111–2119, 1998.

[46] Stephen J. Freeland, Robin D. Knight, Laura F. Landweber, and Laurence D. Hurst. Early fixation of an optimal genetic code. *Molecular Biology and Evolution*, 17(4):511–518, 2000.

[47] Arnaud Denjoy. Sur les courbes définies par les équations différentielles à la surface du tore. *Journal de Mathématiques Pures et Appliquées*, 11:333–375, 1932.

[48] J. F. Koksma. Ein mengentheoretischer satz über die gleichverteilung modulo eins. *Compositio Mathematica*, 2:250–258, 1935.

[49] Ronald L. Graham, Donald E. Knuth, and Oren Patashnik. *Concrete Mathematics: A Foundation for Computer Science*. Addison-Wesley, Reading, MA, 2 edition, 1994.

[50] L. Clozel. The sato-tate conjecture. *Current Developments in Mathematics*, 2006(1):1–34, 2006.

[51] Michael Harris. Galois representations, automorphic forms, and the sato-tate conjecture. *Indian Journal of Pure and Applied Mathematics*, 45(5):707–746, 2014.

[52] Thomas Barnet-Lamb, Toby Gee, and David Geraghty. The sato-tate conjecture for hilbert modular forms. *Journal of the American Mathematical Society*, 24(2), 2011.

[53] Ankit Bisain, Peter Humphries, Andrei Mandelstam, Noah Walsh, and Xun Wang. Subconvexity implies effective quantum unique ergodicity for hecke-maaß cusp forms on $\mathrm{SL}_2(\mathbb{Z})\backslash\mathrm{SL}_2(\mathbb{R})$. *Ens. Number Theory*, 3:101–144, 2024.

[54] Jacob Sturm. On the congruence of modular forms. In *Number Theory (New York, 1984–1985)*, volume 1240 of *Lecture Notes in Mathematics*, pages 275–280. Springer, Berlin, 1987.

[55] N. B. Slater. Gaps and steps for the sequence nθ mod 1. *Proceedings of the Cambridge Philosophical Society*, 63(4):1115–1123, 1967.

[56] Pierre Deligne. La conjecture de weil. i. *Publications Mathématiques de l'Institut des Hautes Études Scientifiques*, 43:273–307, 1974.